Glycolysis-dependent Sulfur Metabolism Orchestrates Morphological Plasticity and Virulence in Fungi

Authors:
Dhrumi Shah[1,2], Nikita Rewatkar[1], Adishree M[1], Siddhi Gupta[1,2], Sudharsan Mathivathanan[1], Sayantani Biswas[1] and Sriram Varahan[1#]

Affiliations:
[1]CSIR-Centre for Cellular and Molecular Biology, Uppal Road, Hyderabad 500007, India.

[2]Academy of Scientific and Innovative Research (AcSIR), Ghaziabad- 201002, India.

- Corresponding Author:
Dr. Sriram Varahan
Senior Scientist
CSIR-Centre for Cellular and Molecular Biology (CCMB)
Email: sriram@ccmb.res.in

Abstract

Fungi exhibit remarkable morphological plasticity, which allows them to undergo reversible transitions between distinct cellular states in response to changes in their environment. This phenomenon, termed fungal morphogenesis, is critical for fungi to survive and colonize diverse ecological niches and establish infections in a variety of hosts. Despite significant advancements in the field with respect to understanding the gene regulatory networks that control these transitions, the metabolic determinants of fungal morphogenesis remain poorly characterized. In this study, we uncover a previously uncharacterized, conserved dependency between central carbon metabolism and *de novo* biosynthesis of sulfur-containing amino acids that is critical for fungal morphogenesis, in two key fungal species. Using a multidisciplinary approach, we demonstrate that glycolytic flux is crucial to drive fungal morphogenesis in a cAMP-independent manner and perturbation of this pathway leads to a significant downregulation in the expression of genes involved in *de novo* biosynthesis of sulfur-containing amino acids. Remarkably, exogenous supplementation of sulfur-containing amino acids robustly rescues the morphogenesis defect induced by the perturbation of glycolysis in both *Saccharomyces cerevisiae* and *Candida albicans*, underscoring the pivotal role of *de novo* biosynthesis of sulfur-containing amino acid as a downstream effector of morphogenesis. Furthermore, a *C. albicans* mutant lacking the glycolytic enzyme, phosphofructokinase (Pfk1) exhibited significantly reduced survival within *murine* macrophages and attenuated virulence in a *murine* model of systemic candidiasis. Overall, our work elucidates a previously uncharacterized coupling between glycolysis and sulfur metabolism that is critical for driving fungal morphogenesis, contributing to our understanding of this conserved phenomenon.

Key words: Fungal Morphogenesis, Glycolysis, *Saccharomyces cerevisiae, Candida albicans,* Virulence

Introduction

In response to changes in their environment, fungi exhibit remarkable morphological plasticity, allowing them to reversibly transition between specialized cell states. This inherent ability to rapidly adapt to the changes in their environment is essential for their survival and allows them to colonize diverse ecological niches including various host organisms (Gow et al., 2002; Lin et al., 2015; Naranjo-Ortiz and Gabaldón, 2019). This conserved phenomenon, of fungal morphogenesis, encompasses a plethora of morphological forms including pseudohyphae and hyphae to name a few (Lin et al., 2015). Importantly, these morphological transitions in various pathogenic fungal species significantly influence their interaction with the respective host, impacting their overall ability to cause persistent infections (Min et al., 2020; Wang and Lin, 2012). Fungal morphogenesis is conserved across a plethora of fungal species and has profound implications with respect to fungal ecology, anti-fungal drug resistance and pathogenicity across a spectrum of hosts (Christensen, 1989; Puumala et al., 2024; Sexton and Howlett, 2006). Consequently, it has been a central focus of intense scientific investigation over the last several years (Lin et al., 2015; Riquelme et al., 2018). During dimorphic transitions in fungi, changes in cell shape is accompanied with changes in cell polarity, cell size and cell-cell adhesion and these changes are regulated by two major signalling pathways: the cAMP-PKA pathway and MAP kinase (MAPK) pathways. Both pathways are crucial for morphogenesis in *Saccharomyces cerevisiae* and *Candida albicans*. The cAMP-PKA pathway acts as a key nutrient sensor; specifically, the presence of glucose activates it to promote pseudohyphal differentiation in *S. cerevisiae* (Xue et al., 1998). Similarly, this pathway drives the essential yeast-to-hyphal transition in *C. albicans*, often *via* the regulator Efg1 (Maidan et al., 2005). Concurrently, the MAPK pathway responds to various environmental stresses and plays a crucial role in regulating fungal morphogenesis. For example, in *S. cerevisiae*, the Kss1 pathway is responsible for driving filamentous growth (Lorenz and Heitman, 1998). Similarly, in *C. albicans*, the Cek1 pathway controls hyphal development and biofilm formation (Csank et al., 1998). The cAMP-PKA and MAPK pathways function in a parallel manner, engaging in significant crosstalk to integrate diverse environmental signals and coordinate a precise morphological response (Biswas et al., 2007; Kumar, 2021). While significant progress has been made in elucidating the intricate gene regulatory networks that govern these morphological transitions (e.g., Genetic networks that orchestrate yeast to pseudohyphal differentiation in *S. cerevisiae* and yeast to hyphal differentiation in *C. albicans* have been well characterized (Nantel et al., 2002; Ryan et al., 2012)), a critical knowledge gap persists regarding the underlying metabolic determinants of fungal morphogenesis. Despite the recognized influence of nutrient availability on fungal morphogenesis (Broach, 2012; Fleck et al., 2011; Kumar, 2021), our understanding of the specific metabolic networks and their regulatory influence on morphogenetic switching in fungi remain incompletely characterized.

In this study, we employed *S. cerevisiae* and the human fungal pathogen, *C. albicans* to dissect the metabolic underpinnings of fungal morphogenesis, under nitrogen-limiting conditions, a known trigger for morphogenetic switching in these fungi (Csank et al., 1998; Gimeno et al., 1992). Our findings reveal a critical role for central carbon metabolism, particularly glycolysis, in facilitating the yeast-to-pseudohyphal transition in *S. cerevisiae* in a cAMP-PKA independent manner and the yeast-to-hyphal transition in *C. albicans*, both of which have been shown to be crucial for their nutrient foraging ability in diverse niches and the ability of *C. albicans* to successfully infect a host (Palková and Váchová, 2006; Thompson et al., 2011). Comparative transcriptomic analysis identified a conserved

metabolic network crucial for these morphogenetic switching events under nitrogen-limiting conditions. Importantly, we observed that perturbations in glycolytic flux using pharmacological and genetic means, negatively impact the expression of genes involved in sulfur metabolism. Furthermore, our functional studies demonstrated that supplementation with sulfur-containing amino acids (cysteine or methionine), effectively rescued the morphogenetic defects resulting from glycolytic impairment, establishing a novel metabolic axis linking glycolysis and sulfur metabolism in the regulation of fungal morphogenesis. Finally, we investigated the implications of this glycolysis-dependent sulfur metabolism on the virulence of *C. albicans*. Our data demonstrates that a *C. albicans* mutant lacking genes that encode for a crucial glycolytic enzyme, phosphofructokinase (Pfk1), exhibits reduced survival within macrophages and severely attenuated virulence in an *in vivo murine* model of systemic candidiasis which is rescued in response to sulfur supplementation to the host.

Collectively, our research, for the first time, identifies a previously uncharacterized metabolic axis linking glycolysis and sulfur metabolism under conditions that induce fungal morphogenesis and underscores the importance of this metabolic network in regulating fungal morphogenesis across two key fungal species and the ability of the human fungal pathogen, *C. albicans* to establish infection in a host. These findings address a fundamental knowledge gap in the field and contributes significantly to our understanding of a broadly conserved phenomenon that exists across a plethora of fungal species.

Results

Glycolysis is Critical for Pseudohyphal Differentiation in a cAMP-PKA Independent Manner in *S. cerevisiae*:

Nitrogen limitation is essential for yeast to pseudohyphal transition in *S. cerevisiae* (Gimeno et al., 1992; Pan et al., 2000). However, the influence of carbon sources on this phenomenon is not completely understood. It has been observed that fermetable carbon sources (sucrose, maltose, glucose, etc.) are important for inducing pseudohyphal differntiation under nitrogen-limiting conditions (Van De Velde and Thevelein, 2008). Conversely, when these were replaced with non-fermentable carbon sources, there was a significant reduction in pseudohyphal differentiation (Strudwick et al., 2010). This indicates that the presence of fermentable carbon sources is critical for pseudohyphal differentiation in *S. cerevisiae*. Crabtree positive organisms like *S. cerevisiae* metabolize glucose primarily *via* glycolysis to meet their growth and energy demands (Barford and Hall, 1979; De Deken, 1966). In order to determine whether the ability of *S. cerevisiae* to metabolize glucose *via* glycolysis is critical for pseudohyphal differentiation under nitrogen-limiting conditions, we spotted *S. cerevisiae* wild-type ∑1278b on nitrogen-limiting media containing 2% glucose (SLAD) with and without sub-inhibitory concentrations of 2-Deoxy-D-Glucose (2DG) and sodium citrate (NaCi), which are well characterized glycolysis inhibitors (Cramer and Woodward, 1952; Evans and Ratledge, 1985; Yoshino and Murakami, 1982) and monitored pseudohyphal differentiation (Fig. 1A). Our data demonstrates that sub-inhibitory concentrations of 2DG and NaCi significantly attenuated the ability of *S. cerevisiae* to undergo pseudohyphal differentiation (Fig. 1B). We then isolated cells from these colonies and quantified the percentage of pseudohyphal cells (cells with a length/width ratio of 2 or more (Schröder et al., 2000)) in these colonies. Addition of 2DG or NaCi resulted in a significant reduction in pseudohyphal cells (Fig. 1C) without compromising the overall growth of *S. cerevisiae* wild-type ∑1278b (Fig. 1G).

199 Another diploid *S. cerevisiae* strain that is known to undergo pseudohyphal differentiation
200 under nitrogen-limiting conditions is the prototrophic CEN.PK strain (Laxman and Tu,
201 2011). In order to determine if our observations in ∑1278b can be recapitulated in CEN.PK,
202 *S. cerevisiae* wild-type CEN.PK was spotted on SLAD with and without sub-inhibitory
203 concentrations of 2-Deoxy-D-Glucose (2DG) and sodium citrate (NaCi). Our data clearly
204 demonstrates that 2DG and NaCi strongly inhibit pseudohyphal differentiation (Fig. 1B and
205 C) without compromising the overall growth of *S. cerevisiae* wild-type CEN.PK as well (Fig.
206 1G).
207
208 Given that, 2DG and NaCi exhibited a strong inhibitory effect on pseudohyphal
209 differentiation under nitrogen-limiting conditions in a strain-independent manner, we
210 wanted to corroborate these observations by using pertinent genetic knockout strains that
211 are compromised in performing glycolysis, in the presence of glucose (Heinisch, 1986;
212 Smith et al., 2004). In order to do this, we generated knockout strains which lack the
213 genes that encode for enzymes that are involved in the glycolysis pathway including *pfk1*
214 (phosphofructokinase-1) and *adh1* (alcohol dehydrogenase-1) (Bennetzen and Hall, 1982;
215 Foy and Bhattacharjee, 1978) (Fig. 1D). Heinisch observed that a null mutant of *pfk1*, a
216 key glycolytic enzyme, is viable and can grow on glucose as a sole carbon source under
217 conditions where cell performs aerobic glycolysis. However, this same mutant exhibits a
218 significant growth defect when cultured anaerobically (Heinisch, 1986; Lobo and Maitra,
219 1983). Similarly, Dickinson et al., showed that a null mutant of *adh1* is viable. This is
220 likely due to the presence of multiple alcohol dehydrogenase isozymes present in *S.*
221 *cerevisiae* that likely compensate for the absence of *adh1*. (Dickinson et al., 2003). The
222 deletions of *pfk1* and *adh1* genes were confirmed through whole genome sequencing
223 (Suppl.Fig. 1A and B). Our result demonstrates that the deletion of *pfk1* and *adh1* in the
224 ∑1278b background (*ΔΔpfk1* refers to the *pfk1* knockout strain and *ΔΔadh1* refers to the
225 *adh1* knockout strain) resulted in a significant reduction in pseudohyphal differentiation,
226 compared to the corresponding wild-type strain, under nitrogen-limiting conditions (Fig.
227 1E). We then isolated cells from these colonies and quantified the percentage of
228 pseudohyphal cells in these colonies. Deletion of *pfk1* and *adh1* resulted in a significant
229 reduction in pseudohyphal cells (Fig. 1F) corroborating our data obtained using the
230 glycolytic inhibitors, 2DG and NaCi. Similarly, deletion of *pfk1* and *adh1* in the CEN.PK
231 background resulted in a significant reduction in pseudohyphal differentiation (Fig. 1E and
232 F). In order to rule out whether the reduction in pseudohyphal differentiation in these
233 mutants, is due to a general growth defect, we performed growth curve analysis wherein
234 overnight grown cultures of the deletion strains (*ΔΔpfk1* and *ΔΔadh1)* along with wild-
235 type strains (∑1278b or CEN.PK) were diluted to OD_{600}=0.01 in fresh SLAD and allowed to
236 grow at 30 °C for 24 hours. OD_{600} was recorded at 3-h intervals (Fig. 1H). Our data
237 suggests that the reduction in pseudohyphal differentiation is not due to general growth
238 defects as the mutants were able to grow similar to the wild-type strains in SLAD (Fig.
239 1H). Taken together, our results clearly demonstrate that the ability of *S. cerevisiae* to
240 efficiently metabolize glucose *via* glycolysis is critical for pseudohyphal differentiation
241 under nitrogen-limiting conditions.
242
243 It is well-established that in *S. cerevisiae*, glucose acts as a key signalling molecule and is
244 sensed by the G-protein-coupled receptor Gpr1 that activates the cAMP-PKA pathway,
245 which in turn is crucial for pseudohyphal differentiation under nitrogen-limiting conditions
246 (Lorenz, 1997; Lorenz et al., 2000). Additionally, a key glycolytic intermediate, fructose-
247 1,6-bisphosphate (FBP), is also known to activate the cAMP-PKA pathway *via* activation of
248 Ras proteins, further linking glucose metabolism to this crucial signalling cascade (Peeters

et al., 2017) (Fig. 1I). To investigate whether the pseudohyphal differentiation defects that we observed due to glycolysis perturbation were solely due to the inability of glucose to activate the cAMP-PKA pathway, we performed cAMP add-back assays wherein *S. cerevisiae* wild-type ∑1278b was spotted on SLAD containing sub-inhibitory concentrations of 2DG or NaCi in the presence and absence of 1mM cAMP (Lorenz, 1997). Interestingly, the exogenous addition of cAMP failed to rescue pseudohyphal differentiation defect caused by the perturbation of glycolysis through 2DG or NaCi under nitrogen-limiting condition (Fig. 1J). We next asked if the exogenous addition of cAMP rescues the pseudohyphal differentiation defect exhibited by glycolysis defective strains, *ΔΔpfk1* and *ΔΔadh1*. In order to do this, we performed similar cAMP add-back assays wherein *S. cerevisiae* wild-type ∑1278b along with *ΔΔpfk1* and *ΔΔadh1* strains were spotted on SLAD in the presence and absence of 1mM cAMP. The *ΔΔgpa2* strain was used as a control because it is well-established that the deletion of *gpa2* (G protein that activates cAMP production in response to glucose (Rolland et al., 2000)) impairs pseudohyphal differentiation and this defect can be fully rescued by the exogenous addition of cAMP under nitrogen-limiting conditions (Harashima and Heitman, 2002; Lorenz, 1997). Corroborating our previous data, the exogenous addition of cAMP failed to rescue pseudohyphal differentiation defect caused by the perturbation of glycolysis *via* the deletion of *pfk1* and *adh1* but fully rescued the pseudohyphal differentiation defect exhibited by the *ΔΔgpa2* strain (Fig. 1K). Taken together, our results clearly demonstrate that the ability of *S. cerevisiae* to efficiently metabolize glucose *via* glycolysis is critical for pseudohyphal differentiation in a cAMP-PKA pathway independent manner under nitrogen-limiting conditions. This implies that glycolysis may be parallelly regulating other cellular processes essential for this morphological transition under nitrogen-limiting conditions.

Comparative Transcriptomics Identifies Glycolysis-dependent Regulation of Sulfur Metabolism During Pseudohyphal Differentiation in *S. cerevisiae*:

Our previous data showed that the perturbation of glycolysis using specific inhibitors including 2DG/NaCi or deletion of genes that encode for glycolytic enzymes including *pfk1/ adh1* resulted in a significant reduction in pseudohyphal differentiation in a cAMP-PKA independent manner, under nitrogen-limiting conditions (Fig. 1). Given that, glycolysis strongly influences the global transcriptional landscape of *S. cerevisiae* (Newcomb et al., 2003; Wu et al., 2019), we undertook a comprehensive transcriptomic approach to identify the changes in the transcriptional landscape of *S. cerevisiae* colonies, in conditions that perturb glycolysis, resulting in the inhibition of pseudohyphal differentiation. We performed comparative RNA-Seq analysis using RNA isolated from wild-type cells spotted on SLAD in the presence and absence of the glycolysis inhibitor, 2DG (2DG addition was used to perturb glycolysis in our transcriptomics experiments, as it exerted the strongest inhibitory effect on pseudohyphal differentiation as shown in Fig. 1B and C). The experimental schematic is depicted in Fig. 2A. Briefly, comparative RNA-Seq analysis was done using wild-type colonies grown on SLAD in the presence and absence of 2DG isolated on day 5 (D-5) and day 10 (D-10), respectively (Fig. 2A). We have used D-5 as an early time point for our experiments, as we have consistently observed the emergence of pseudohyphae in colonies spotted on SLAD at this time-point and D-10 as a late time point wherein colonies exhibit robust pseudohyphal differentiation (Suppl.Fig. 2A). A volcano plot of differential gene expression in 2DG treated cells compared to untreated cells in both D-5 and D-10 is shown in Fig. 2B wherein some of the significantly upregulated and downregulated genes are highlighted with green colour. Previous studies in the field have shown that, under nitrogen-limiting/glucose-replete conditions, glycolytic intermediates

provide various precursors needed for the biosynthesis of several amino acids in order to maintain amino acid homeostasis (Dikicioglu et al., 2011; Martíez-force and Benítez, 1992) and perturbation of glycolysis under these conditions results in the increased transcription of various genes involved in amino acid biosynthesis, as a feedback response. As expected, the expression of several genes involved in amino acid biosynthesis and transport were significantly upregulated in 2DG treated cells compared to untreated cells, in both D-5 and D-10 respectively (Suppl.Fig. 2B) corroborating the observations from the previously mentioned studies (Dikicioglu et al., 2011; Wu et al., 2004). Interestingly and rather unexpectedly, the expression of multiple genes specifically involved in the biosynthesis and transport of sulfur-containing amino acids, cysteine and methionine were significantly downregulated in 2DG treated cells compared to untreated cells in both D-5 and D-10 respectively (Fig.2C). Our RNA-Seq analysis clearly demonstrates that multiple genes involved in the de novo biosynthesis of sulfur-containing amino acids, are significantly downregulated in the presence of 2DG, under nitrogen-limiting conditions. In order to determine whether these observed trends are reflected at the protein level, we generated strains wherein various proteins involved in the de novo biosynthesis of sulfur-containing amino acids including Met4 (Leucine-zipper transcriptional activator), Met32 (Zinc-finger DNA-binding transcription factor), Met16 (3'-phosphoadenylsulfate reductase), Met10 (Subunit alpha of assimilatory sulfite reductase), Cys4 (Cystathionine beta-synthase) and Cys3 (Cystathionine gamma-lyase) were epitope-tagged (Fig. 2D). These strains were spotted on SLAD in the presence and absence of 2DG following which, cells from colonies were isolated on D-5 and levels of these proteins were assessed by using Western blotting (Fig. 2E). Our results indicate that the levels of Met4, Met32, Met16, Met10, Cys4 and Cys3 were significantly reduced in the 2DG treated cells compared to untreated cells, corroborating our transcriptome data (Fig. 2E and Suppl.Fig. 3A). This clearly demonstrates that perturbation of glycolysis negatively influences the expression of sulfur metabolism proteins, under nitrogen-limiting conditions. We next asked, if the glycolysis-dependent regulation of sulfur metabolism under nitrogen-limiting conditions (SLAD) is restricted to conditions wherein cells physically attach to solid surfaces (colony growth) or whether it is conserved even in conditions where cells are free-floating (liquid-culture growth). In order to do this, pertinent epitope-tagged strains (wherein Met32, Met16, Met10 and Cys3 were HA-tagged) were grown in liquid SLAD in the presence and absence of 2DG for 24 hours after which the expression of the aforesaid proteins were assessed using Western blotting (Suppl.Fig. 3B and C). Importantly, our results indicate that the levels of Met32, Met16, Met10 and Cys3 were significantly reduced in the 2DG treated cells compared to untreated cells (Suppl.Fig. 3B and C). Taken together, our data clearly demonstrates that the perturbation of glycolysis under nitrogen-limiting conditions negatively influences sulfur metabolism.

Exogenous Supplementation of Sulfur Sources Rescues Pseudohyphal Differentiation Defects Caused by the Perturbation of Glycolysis in *S. cerevisiae*:

Our comparative transcriptomics data clearly demonstrates that, under nitrogen-limiting conditions, glycolysis plays a critical role in regulating the expression of genes involved in the *de novo* biosynthesis of sulfur-containing amino acids (Fig. 2). Based on our previous data, we hypothesized that under nitrogen-limiting conditions, active glycolysis enables *de novo* biosynthesis of sulfur-containing amino acids which in turn, is critical for pseudohyphal differentiation and perturbation of active glycolysis using inhibitors like 2DG or disruption of genes involved in glycolysis including *pfk1* or *adh1* negatively affects glycolysis-mediated regulation of sulfur metabolism leading to attenuation of

349 pseudohyphal differentiation. If the proposed hypothesis holds true, the exogenous
350 supplementation of sulfur-containing compounds should mitigate the fungal
351 morphogenetic defects resulting from the perturbation of glycolysis. In order to test this,
352 we performed sulfur add-back assays wherein *S. cerevisiae* wild-type ∑1278b was spotted
353 on SLAD containing sub-inhibitory concentration of 2DG in the presence and absence of
354 either sulfur-containing amino acids (cysteine or methionine). Remarkably, the exogenous
355 addition of cysteine resulted in a significant rescue of the pseudohyphal differentiation
356 defect observed in nitrogen-limiting medium containing 2DG (Fig. 3A). Corroborating this
357 observation, the percentage of pseudohyphal cells in colonies isolated from SLAD
358 containing 2DG and cysteine were significantly higher than the percentage of
359 pseudohyphal cells in colonies isolated from SLAD containing 2DG alone (Fig. 3B),
360 Interestingly, the addition of methionine failed to rescue the pseudohyphal differentiation
361 defects caused by the perturbation of glycolysis (Fig. 3A and B).
362
363 We next asked if the exogenous addition of sulfur sources rescues the pseudohyphal
364 differentiation defect exhibited by glycolysis defective strains, *ΔΔpfk1* and *ΔΔadh1*. In
365 order to do this, we performed similar sulfur add-back assays wherein *S. cerevisiae* wild-
366 type ∑1278b along with *ΔΔpfk1* and *ΔΔadh1* strains were spotted on SLAD in the presence
367 and absence of either sulfur-containing amino acids (cysteine or methionine). The
368 exogenous addition of both cysteine or methionine was able to completely rescue the
369 pseudohyphal differentiation defect exhibited by the *ΔΔpfk1* and *ΔΔadh1* strains (Fig. 3C).
370 Corroborating this observation, the percentage of pseudohyphal cells in *ΔΔpfk1* and
371 *ΔΔadh1* colonies isolated from SLAD containing cysteine or methionine were significantly
372 higher than the percentage of pseudohyphal cells in *ΔΔpfk1* and *ΔΔadh1* colonies isolated
373 from SLAD alone (Fig. 3D). Taken together, our results clearly demonstrate that the
374 glycolysis-mediated regulation of sulfur metabolism is critical for pseudohyphal
375 differentiation under nitrogen-limiting conditions.
376
377 **Sulfur Metabolism is Critical for Pseudohyphal Differentiation Under Nitrogen-**
378 **limiting Conditions in *S. cerevisiae*:**
379
380 Our previous observations strongly suggest a direct role for sulfur metabolism in regulating
381 fungal morphogenesis, under nitrogen-limiting conditions. In order to determine whether
382 glycolysis-dependent sulfur metabolism is critical for pseudohyphal differentiation, under
383 nitrogen-limiting conditions, we generated a knockout strain that lacks *met32* (gene that
384 encodes for a zinc-finger DNA-binding transcription factor involved in the regulation of *de*
385 *novo* biosynthesis of sulfur-containing amino acids). Unlike deletions of most other genes
386 involved in the *de novo* biosynthesis of sulfur-containing amino acids, *met32* deletion
387 strain does not exhibit auxotrophy for methionine or cysteine (Blaiseau et al., 1997). This
388 is likely due to the functional redundancy provided by its paralog, *met31* (Blaiseau et al.,
389 1997). We then assessed the ability of the *met32* deletion strain to undergo pseudohyphal
390 differentiation under nitrogen-limiting conditions. Deletion of *met32* resulted in a
391 significant reduction in pseudohyphal differentiation. Corroborating this observation, the
392 percentage of pseudohyphal cells in *ΔΔmet32* colonies were significantly lower in SLAD,
393 compared to *S. cerevisiae* wild-type ∑1278b colonies (Fig. 3E). This suggests that
394 perturbations to sulfur metabolism negatively affects pseudohyphal differentiation. In
395 order to rule out whether the reduction in pseudohyphal differentiation in this mutant, is
396 due to a general growth defect, we performed growth curve analysis wherein overnight
397 grown cultures of deletion strain (*ΔΔmet32)* along with wild-type strain (∑1278b) were
398 diluted to OD_{600}=0.01 in fresh SLAD and allowed to grow at 30 °C for 24 hours. OD_{600} was

399 recorded at 3-h intervals (Suppl.Fig. 4A). Our data suggests that the reduction in
400 pseudohyphal differentiation is not due to general growth defect as the mutant was able
401 to grow similar to the wild-type strain in SLAD. We next asked if the exogenous addition
402 of sulfur sources rescues the pseudohyphal differentiation defect exhibited by *ΔΔmet32*.
403 In order to do this, we performed a simple sulfur add-back assay, wherein *ΔΔmet32* strain
404 was spotted on SLAD containing either cysteine or methionine and allowed to undergo
405 pseudohyphal differentiation. Our results show that the addition of cysteine or methionine
406 completely rescued the pseudohyphal differentiation defect exhibited by *ΔΔmet32* strain.
407 The percentage of pseudohyphal cells were also significantly higher in *ΔΔmet32* colonies
408 growing on SLAD containing cysteine or methionine compared to just SLAD (Fig. 3F).
409 Taken together, our data clearly demonstrates that the efficient *de novo* biosynthesis of
410 sulfur-containing amino acids including cysteine and methionine is critical for
411 pseudohyphal differentiation, under nitrogen-limiting conditions.
412
413 **Met30 is Involved in the Glycolysis-dependent Regulation of Sulfur Metabolism**
414 **During Pseudohyphal Differentiation in *S. cerevisiae*:**
415
416 Our previous data clearly demonstrates that, under nitrogen-limiting conditions, the levels
417 of Met4, a key activator of genes involved in the *de novo* biosynthesis of sulfur-containing
418 amino acids, was significantly reduced in 2DG treated cells compared to untreated cells
419 (Fig. 2E). Met4 activity is known to be negatively regulated by SCF^{Met30} ubiquitin ligase
420 complex in *S. cerevisiae* (Rouillon et al., 2000). Under sulfur-replete conditions, Met30
421 promotes Met4 ubiquitination and degradation, thereby repressing the *Met* gene network.
422 Conversely, sulfur limitation reduces Met30 activity, allowing Met4 to become active and
423 induce the expression of genes required for sulfur amino acid biosynthesis (Smothers et
424 al., 2000). It is important to note that deletion of *met30* is lethal in haploid strains of
425 *S. cerevisiae* (Kaiser et al., 1998). While point mutations or temperature sensitive *met30*
426 mutants are commonly used in haploid strains to circumvent this lethality (Kaiser et al.,
427 1998; Su et al., 2008), our study in diploid *S. cerevisiae* involved generating a
428 heterozygous viable *met30* (*Δmet30*) deletion strain. Based on our previous data, we
429 hypothesized that under nitrogen-limiting conditions, active glycolysis enables *de novo*
430 biosynthesis of sulfur-containing amino acids by reducing the activity of Met30.
431 Conversely, we hypothesized that perturbing active glycolysis with inhibitors like 2DG
432 increases Met30 activity, which in turn inactivates Met4, thereby negatively affecting *Met*
433 gene transcription, ultimately resulting in attenuated pseudohyphal differentiation (Fig.
434 3G). In order to investigate this hypothesis, we generated strains wherein one copy of
435 *met30* was deleted and various proteins involved in the *de novo* biosynthesis of sulfur-
436 containing amino acids including Met4 (Leucine-zipper transcriptional activator), Met32
437 (Zinc-finger DNA-binding transcription factor), Met16 (3'-phosphoadenylsulfate reductase)
438 and Cys3 (Cystathionine gamma-lyase) were epitope-tagged. These strains were spotted
439 on SLAD in the presence and absence of 2DG following which, cells from colonies were
440 isolated on D-5 and levels of these proteins were assessed by using Western blotting. Our
441 results indicate that the levels of Met4, Met32, Met16 and Cys3 were similar in both 2DG
442 treated and untreated cells, in the *Δmet30* deletion strain (Fig. 3H and I). This suggests
443 that glycolysis influences Met30 activity which in turn regulates Met4 activity thereby
444 affecting the expression of genes involved in the *de novo* biosynthesis of sulfur-containing
445 amino acids, under nitrogen-limiting conditions.
446

447 Based on our previous observation that 2DG treatment significantly reduces Met4 levels
448 in nitrogen-limiting conditions, (an effect that was notably absent in *met30* deletion
449 strains), we hypothesized that the 2DG-induced downregulation of Met4 is mediated by
450 an increase in Met30 levels. In order to check Met30 levels in the presence of 2DG, we
451 generated a strain wherein Met30 was epitope-tagged and this strain was spotted on
452 SLAD, in the presence and absence of 2DG following which, cells from colonies were
453 isolated on D-5 and levels of Met30 were assessed by using Western blotting. Our results
454 indicate that the levels of Met30 were similar in both 2DG treated and untreated cells (Fig.
455 3J), suggesting that glycolysis influences Met30 activity post-translationally rather than
456 through changes in its protein abundance. Collectively, our findings indicate that the
457 perturbation of glycolysis under nitrogen-limiting conditions negatively impacts sulfur
458 metabolism through a mechanism dependent on Met30 activity.
459
460 **Glycolysis-dependent Sulfur Metabolism is Critical for Hyphal Differentiation in**
461 ***C. albicans*:**
462
463 *C. albicans* is an opportunistic fungal pathogen that exhibits a remarkable degree of fungal
464 morphogenesis in response to various environmental cues (Huang, 2012). Yeast to hyphal
465 differentiation in *C. albicans* is well studied. However, we do not have a complete
466 understanding of fundamental metabolic drivers that orchestrate this phenomenon. Given
467 that central carbon metabolic pathways including glycolysis are well conserved across a
468 plethora of fungal species including *C. albicans* (Askew et al., 2009) and nitrogen limitation
469 is one of the key triggers for yeast to hyphal differentiation in *C. albicans* (Csank et al.,
470 1998), we wanted to determine if glycolysis-mediated sulfur metabolism plays an
471 important role in this morphogenetic switching in *C. albicans* as well. First, we wanted to
472 understand whether the ability of C. *albicans* cells to metabolize glucose, under nitrogen-
473 limiting conditions is critical for fungal morphogenesis (Fig. 4A). In order to do this,
474 *C. albicans* wild-type SC5314 was spotted on SLAD, in the presence and absence of sub-
475 inhibitory concentration of glycolysis inhibitor, 2DG, allowed to grow for 7 days, and cells
476 were isolated and imaged using bright-field microscopy. Our data clearly demonstrates
477 that sub-inhibitory concentration of 2DG significantly reduced filamentation in *C. albicans*
478 (Fig. 4B) without compromising the overall growth of *C. albicans* wild-type SC5314 (Fig.
479 4H). We then isolated cells from these colonies and quantified the percentage of hyphal
480 cells (cells with a length/width ratio of 4.5 or more (Su et al., 2018)) in these colonies.
481 Corroborating our microscopy data, the percentage of hyphal cells in colonies spotted on
482 SLAD containing 2DG was significantly lower compared to the percentage of hyphal cells
483 in colonies spotted on SLAD without 2DG (Fig. 4B). Taken together, our results show that
484 the ability of *C. albicans* to metabolize glucose is critical for fungal morphogenesis.
485
486 Given that the perturbation of glycolysis under nitrogen-limiting conditions, using 2DG
487 exhibited a strong inhibitory effect on hyphal differentiation in *C. albicans* (Fig. 4B), similar
488 to what we observed in *S. cerevisiae*, we wanted to determine if the expression of genes
489 involved in the *de novo* biosynthesis of sulfur-containing amino acids are affected when
490 glycolysis is perturbed in *C. albicans*, under nitrogen-limiting conditions (similar to what
491 we observed in *S. cerevisiae*) (Chebaro et al., 2017). In order to determine this, we
492 spotted *C. albicans* wild-type SC5314 on SLAD, in the presence and absence of 2DG and
493 cells from colonies were isolated after ~4 days for RNA isolation. We then performed
494 comparative RT-qPCR to check for the relative expression of genes involved in *de novo*
495 biosynthesis of sulfur-containing amino acids including *met32* (DNA-binding transcription
496 factor), *met3* (ATP sulfurylase), *met5* (*ecm17*) (Sulfite reductase beta subunit), *met10*

497 (Sulfite reductase), and *met17* (*met15*) (O-acetyl homoserine-O-acetyl serine
498 sulfhydrylase) (Chebaro et al., 2017; Li et al., 2013; Shrivastava et al., 2021), in cells
499 isolated from colonies grown on SLAD containing 2DG compared to cells isolated from
500 colonies grown on SLAD without 2DG (Fig. 4C). Our data clearly shows that all the
501 aforesaid genes involved in *de novo* biosynthesis of sulfur-containing amino acids pathway
502 including *met32*, *met3*, *met5* (*ecm17*), *met10* and *met17* (*met15*) were significantly
503 downregulated in the presence of 2DG (Fig. 4D) suggesting that perturbation of glycolysis
504 negatively impacts sulfur metabolism in *C. albicans*, under nitrogen-limiting conditions. To
505 determine if the significant reduction in hyphal differentiation that we observed in the
506 presence of 2DG can be attributed to the reduced expression of genes involved in the *de*
507 *novo* biosynthesis of sulfur-containing amino acids, we performed sulfur add-back assays
508 similar to what was done in *S. cerevisiae* (Fig. 3A), wherein *C. albicans* wild-type SC5314
509 was spotted on SLAD containing 2DG in the presence and absence of cysteine and
510 methionine, allowed to grow for 7 days, and cells were isolated and imaged using bright-
511 field microscopy. The addition of cysteine and methionine significantly rescued hyphal
512 differentiation defects in the presence of 2DG (Fig. 4E and F). We then isolated cells from
513 these colonies and quantified the percentage of hyphal cells. Corroborating our microscopy
514 data, the percentage of hyphal cells in colonies spotted on SLAD containing 2DG with
515 cysteine or methionine were significantly higher compared to the percentage of hyphal
516 cells in colonies spotted on SLAD with 2DG alone (Fig. 4E and F).
517
518 Our previous results clearly demonstrate that glycolysis and glycolysis-dependent sulfur
519 metabolism is critical for fungal morphogenesis of *C. albicans*, under nitrogen-limiting
520 conditions. In order to corroborate these observations by using pertinent genetic knockout
521 strains that are compromised in performing glycolysis, we generated a double knockout
522 strain lacking the gene that encodes for the glycolytic enzyme, phosphofructokinase (Pfk1)
523 using the SAT-Flipper method (Reuß et al., 2004). The deletion of *pfk1* was confirmed
524 through whole genome sequencing (Suppl.Fig. 5A). We then tested the ability of this
525 deletion strain to undergo hyphal differentiation under nitrogen-limiting conditions. Briefly,
526 *C. albicans* wild-type SC5314 and *ΔΔpfk1* were spotted on SLAD, allowed to grow for 7
527 days, and cells were isolated and imaged using bright-field microscopy. Our result shows
528 that the *ΔΔpfk1* strain exhibits a significant reduction in hyphal differentiation compared
529 to *C. albicans* wild-type SC5314, under nitrogen-limiting conditions (Fig. 4G). We then
530 isolated cells from these colonies and quantified the percentage of hyphal cells in these
531 colonies. Corroborating our microscopy data, the percentage of hyphal cells in *C. albicans*
532 wild-type SC5314 colonies spotted on SLAD were significantly higher compared to the
533 percentage of hyphal cells in *ΔΔpfk1* colonies (Fig. 4G). In order to rule out whether the
534 reduction in hyphal differentiation in this mutant, is due to a general growth defect, we
535 performed growth curve analysis wherein overnight grown cultures of deletion strain
536 (*ΔΔpfk1)* along with wild-type strain (SC5314) were diluted to OD_{600}=0.01 in fresh SLAD
537 and allowed to grow at 30 °C for 24 hours. OD_{600} was recorded at 3-h intervals.Our data
538 suggests that the reduction in hyphal differentiation is not due to general growth defects
539 as the mutant was able to grow similar to the wild-type strain in SLAD (Fig. 4H).
540
541 In order to determine if the expression of genes involved in the *de novo* biosynthesis of
542 sulfur-containing amino acids are affected in *ΔΔpfk1*, under nitrogen-limiting conditions
543 (similar to what we observed in the presence of 2DG (Fig. 4D)), we spotted *C. albicans*
544 wild-type SC5314 and *ΔΔpfk1* on SLAD and cells from colonies were isolated after ~4
545 days, for RNA isolation. We then performed comparative RT-qPCR to check for the relative
546 expression of genes involved in *de novo* biosynthesis of sulfur-containing amino acids

547 including *met32* (DNA-binding transcription factor), *met3* (ATP sulfurylase), *met5* (*ecm17*)
548 (Sulfite reductase beta subunit), *met10* (Sulfite reductase) and *met17* (*met15*) (O-acetyl
549 homoserine-O-acetyl serine sulfhydrylase) (Chebaro et al., 2017; Li et al., 2013;
550 Shrivastava et al., 2021)(Fig. 4C). Our data clearly shows that all the aforesaid genes
551 involved in *de novo* biosynthesis of sulfur-containing amino acids pathway including
552 *met32*, *met3*, *met5* (*ecm17*), *met10* and *met17* (*met15*) were significantly downregulated
553 in *ΔΔpfk1* compared to the wild-type (Fig. 4I) suggesting that the genetic perturbation of
554 glycolysis negatively impacts sulfur metabolism in *C. albicans*, under nitrogen-limiting
555 conditions.
556
557 Our RT-qPCR results showed that the, deletion of *pfk1*, negatively influences sulfur
558 metabolism and this in turn might be causal for the reduced hyphal differentiation
559 observed in these conditions. Given this, we wanted to determine if the hyphal
560 differentiation defect exhibited by *ΔΔpfk1* can be rescued by the addition of sulfur-
561 containing amino acids. In order to do this, we performed sulfur add-back assays wherein
562 *ΔΔpfk1* strain was spotted on SLAD in the presence and absence of cysteine and
563 methionine, allowed to grow for 7 days and imaged using bright field microscopy.
564 Interestingly, our data shows that cysteine and methionine were able to rescue the hyphal
565 differentiation defect exhibited by the *ΔΔpfk1* strain (Fig. 4J and K). We then isolated cells
566 from these colonies and quantified the percentage of hyphal cells. Corroborating our
567 microscopy data, the percentage of hyphal cells in *ΔΔpfk1* colonies spotted on SLAD
568 containing cysteine and methionine were significantly higher compared to the percentage
569 of hyphal cells in *ΔΔpfk1* colonies spotted on SLAD alone (Fig. 4J and K). Overall, our data
570 suggests that glycolysis-mediated regulation of sulfur metabolism is critical for hyphal
571 differentiation of *C. albicans*, under nitrogen-limiting conditions highlighting the
572 remarkable similarities with respect to the regulation of fungal morphogenesis, between
573 *S. cerevisiae* and *C. albicans*.
574
575 **Perturbation of Glycolysis Leads to Attenuated Fungal Virulence in *C. albicans***
576 **which is Rescued by Sulfur Supplementation:**
577
578 Several studies have established the importance of fungal morphogenesis as a key
579 virulence strategy used by *C. albicans* to establish successful infections in the host
580 (Gow et al., 2012; Moyes et al., 2016; Wilson et al., 2016). Based on our previous
581 observations that perturbation of glycolysis, either through 2DG treatment or deletion of
582 *pfk1* (*ΔΔpfk1*), significantly attenuates hyphal differentiation, we hypothesized that this
583 observed phenotype could be a consequence of transcriptional downregulation of genes
584 associated with hyphal differentiation and virulence. In order to test this hypothesis, we
585 spotted *C. albicans* wild-type SC5314 on SLAD, in the presence and absence of 2DG or
586 wild-type along with *ΔΔpfk1* on SLAD. Cells from colonies were isolated after ~4 days for
587 RNA isolation. We then performed comparative RT-qPCR to check for the relative
588 expression of genes involved in hyphal differentiation and virulence including *als3* (Cell
589 wall adhesin), *ece1* (Candidalysin), *hwp1* (Hyphal cell wall protein), *hyr1* (GPI-anchored
590 hyphal cell wall protein), *ihd1* (GPI-anchored protein), *rbt1* (Cell wall protein) and *sap6*
591 (Secreted aspartyl protease) (Bailey et al., 1996; Deorukhkar, 2017; Liu and Filler, 2011;
592 Martin et al., 2013; Monniot et al., 2013; Moyes et al., 2016; Richardson et al., 2018;
593 Sharkey et al., 1999) (Fig. 5A). Our data clearly shows that all the aforesaid genes involved
594 in hyphal differentiation and virulence including *als3, ece1, hwp1, hyr1, ihd1, rbt1* and
595 *sap6* were significantly downregulated in both 2DG treated cells and in *ΔΔpfk1* suggesting

596 that perturbation of glycolysis negatively affects the expression of genes involved in hyphal
597 differentiation and virulence in *C. albicans*, under nitrogen-limiting conditions (Fig. 5B).
598
599 Given that *ΔΔpfk1*, displayed a significant attenuation in its ability to undergo hyphal
600 differentiation and it had significantly reduced expression of genes associated with hyphal
601 differentiation and virulence, we wanted to determine if this deletion strain was
602 compromised in its ability to infect the host. In order to do this, we took a two-pronged
603 approach wherein, we first tested the ability of the *ΔΔpfk1* strain to survive the harsh
604 intracellular environment of the macrophages which *C. albicans* encounters during various
605 stages of host infection (Jiménez-López and Lorenz, 2013; May and Casadevall, 2018;
606 Uwamahoro et al., 2014). We performed an *in vitro* microbial survival assay wherein *RAW*
607 *264.7* macrophages were incubated either with *C. albicans* wild-type SC5314 or the
608 *ΔΔpfk1* strain for one hour following which macrophages were lysed and fungi were serially
609 diluted and plated to determine the viable population of the *C. albicans* wild-type SC5314
610 and the *ΔΔpfk1* strain (Fig. 5C). We also calculated the percentage of the wild-type or
611 mutant strain that survived the incubation with the macrophages. Our results demonstrate
612 that the viable population of *ΔΔpfk1* strain was significantly lower compared to the wild-
613 type strain, after incubation with the macrophages (Fig. 5C). Similarly, the percentage
614 survival of the *ΔΔpfk1* strain was significantly lower than the wild-type strain (Fig. 5C).
615 Overall, this data indicates that the *ΔΔpfk1* strain is compromised with respect to
616 macrophage survival.
617
618 Given that the *ΔΔpfk1* strain was significantly attenuated in the macrophage survival
619 assay, we next wanted to test the ability of this deletion strain to establish systemic
620 infection in a host. In order to do this, we challenged healthy wild-type C57BL/6 mice
621 intravenously with a dose of 1×10^7 CFU (lethal dose (Hirayama et al., 2020)) of
622 *C. albicans* wild-type SC5314 or *ΔΔpfk1* strain *via* lateral tail vein injection. This is an
623 established *murine* model of systemic candidiasis in the field and faithfully mimics the
624 infection that occurs in humans (Segal and Frenkel, 2018). We then monitored survival of
625 the infected animals for 21 days. Mice challenged with *ΔΔpfk1* strain had significantly
626 increased survival compared to mice challenged with *C. albicans* wild-type SC5314 (Fig.
627 5D). *C. albicans* exhibits strong tropism towards kidneys during *murine* infections (Lionakis
628 et al., 2011; Pappas et al., 2018) and in order to measure the fungal burden within the
629 host, kidneys from C57BL/6 mice infected with both *C. albicans* wild-type SC5314 and
630 *ΔΔpfk1* were harvested ~2 days post infection (when the mice injected with wild-type
631 *C. albicans* SC5314 becomes moribund), homogenized and plated to measure the fungal
632 burden by enumerating the colony forming units (CFU) (Fig. 5E). Our data indicates that
633 kidneys isolated from mice challenged with the *ΔΔpfk1* strain had significantly lesser CFU
634 compared to kidneys isolated from mice challenged with the *C. albicans* wild-type SC5314
635 (Fig. 5F). We also performed histological analysis on the infected kidneys using GMS
636 staining (Grocott Methenamine Silver staining), to visualize the fungi (stained black) in
637 the tissue. Kidneys isolated from mice challenged with the *C. albicans* wild-type SC5314
638 had higher amounts of fungi compared to kidneys isolated from mice challenged with the
639 *ΔΔpfk1* strain (Fig. 5G). Overall, our data indicates that the perturbation of glycolysis
640 significantly attenuates *C. albicans* virulence.
641
642 Our previous *in vitro* results clearly demonstrated that exogenous supplementation of
643 cysteine and methionine significantly rescued the hyphal differentiation defect exhibited
644 by *ΔΔpfk1* strain. Based on this, we wanted to check whether sulfur supplementation could
645 also rescue the virulence defects exhibited by *ΔΔpfk1*, in a *murine* model of systemic

candidiasis. Given that N-acetyl cysteine (NAC) is a commonly used exogenous sulfur source for *in vivo* studies (Shee et al., 2022), we supplemented distilled water with NAC (6mg/ml concentration) and this was administered to mice orally 72 hours prior to infection. After 72 hours of pre-treatment with NAC, we challenged healthy wild-type C57BL/6 mice intravenously with a dose of 1×10^7 CFU of wild-type SC5314 or *ΔΔpfk1* strain *via* lateral tail vein injection (Fig. 5H). We then monitored survival of the infected animals for 21 days. Remarkably, mice administered with NAC containing distilled water had significantly reduced survival compared to mice administrated with normal distilled water (Fig. 5I). We also performed histological analysis on the infected kidneys using GMS staining, to visualize the fungi in the tissue. Kidneys isolated from mice administered with NAC containing distilled water and infected with *ΔΔpfk1* had significantly higher amounts of fungi compared to mice administrated with normal distilled water (Fig. 5J). This clearly demonstrates that exogenous sulfur supplementation to the host *via* NAC administration, reverses the attenuated virulence exhibited by the *ΔΔpfk1* strain.

Discussion

Our findings provide compelling evidence for a conserved metabolic network that intricately links central carbon metabolism (particularly glycolysis), sulfur amino acid biosynthesis, and fungal morphogenesis in both *Saccharomyces cerevisiae* and *Candida albicans*. While nitrogen limitation is a well-established and essential trigger for the yeast-to-pseudohyphae transition in *S. cerevisiae*, the specific influence of carbon sources on this process has not been completely understood. Studies have shown that fermentable carbon sources are critical for inducing pseudohyphal differentiation under nitrogen-limiting conditions (Van De Velde and Thevelein, 2008). Conversely, when these fermentable sugars are replaced with non-fermentable carbon sources, a significant reduction in pseudohyphal differentiation is observed (Strudwick et al., 2010). These findings collectively suggest that the presence of fermentable carbon sources, and by extension their metabolism, is a critical requirement for inducing fungal morphogenesis in *S. cerevisiae*. Glucose in the extracellular environment can be sensed by *S. cerevisiae* using multiple proteins. One such protein is the well characterized G-Protein Couple Receptor (GPCR), Gpr1. Binding of glucose to Gpr1 activates a downstream signalling cascade, resulting in the production of cAMP which activates Protein Kinase A (PKA) (Kraakman et al., 1999; Yun et al., 1997). This glucose-dependent cAMP-PKA pathway has been shown to be essential for pseudohyphal differentiation under nitrogen-limiting conditions (Lorenz et al., 2000). Additionally, a key glycolytic intermediate, fructose-1,6-bisphosphate (FBP), is also known to activate the cAMP-PKA pathway *via* activation of Ras proteins, further linking glucose metabolism to this crucial signalling cascade. However, the role of glucose as a metabolite in the context of pseudohyphal differentiation is not known. Building upon previous data that fermentable carbon sources that are metabolized *via* glycolysis are able to robustly induce fungal morphogenesis, we asked whether the ability of these cells to undergo active glycolysis is critical for fungal morphogenesis. We took a two-pronged approach which involved pharmacological or genetic perturbation of glycolysis, to address this question. Perturbation of glycolysis using sub-inhibitory concentrations of well-characterized inhibitors (Cramer and Woodward, 1952; Yoshino and Murakami, 1982), 2DG or NaCi significantly attenuated pseudohyphal differentiation in both *S. cerevisiae* strains (∑1278b and CEN.PK) that are known to undergo pseudohyphal differentiation, without compromising overall growth. This strain-independent effect was further corroborated by genetic evidence wherein deletion of key glycolytic enzyme-encoding genes, *pfk1* and *adh1*, in both the strain backgrounds (∑1278b and CEN.PK) also

resulted in a significant reduction in pseudohyphal differentiation, without causing general growth defects. These convergent findings strongly support the notion that active glycolysis is essential for fungal morphogenesis under nitrogen-limiting conditions. To understand whether the pseudohyphal differentiation defects we observed due to glycolysis perturbation were solely due to the inability of glucose to activate glucose-dependent cAMP-PKA pathway, we performed cAMP add-back assays and interestingly, exogenous supplementation of cAMP failed to rescue pseudohyphal differentiation defects caused by the perturbation of glycolysis (through inhibitors (2DG and NaCi) or through genetic knockout strains (*ΔΔpfk1* and *ΔΔadh1*)). Our results clearly demonstrate that the ability of *S. cerevisiae* to efficiently metabolize glucose *via* glycolysis is critical for pseudohyphal differentiation under nitrogen-limiting conditions, in a cAMP-PKA independent manner. This implies that glycolysis may be parallelly regulating other cellular mechanisms essential for this morphological transition. It is plausible that the glycolytic flux, or a yet to be identified downstream intermediate, acts as a distinct metabolic signal that is parallelly important for pseudohyphal differentiation along with the cAMP-PKA pathway. This uncovers a previously unrecognized layer of regulatory complexity in the interplay between central carbon metabolism and fungal morphogenesis.

To gain deeper insights underlying the glycolysis-mediated regulation of fungal morphogenesis in a cAMP-PKA independent manner, we performed comparative transcriptomics on *S. cerevisiae* wild-type cells grown under nitrogen-limiting conditions with and without the glycolysis inhibitor 2DG (which had the strongest inhibitory effect on pseudohyphal differentiation). As anticipated, genes involved in amino acid biosynthesis and transport were upregulated in the 2DG treated cells, consistent with a feedback response that cells exhibits when glycolysis is perturbed under nitrogen-limiting conditions, as various intermediates of glycolysis are known to serve as precursors for the biosynthesis of several amino acids under these conditions (Dikicioglu et al., 2011; Martíez-force and Benítez, 1992). Remarkably, we observed a striking and unexpected downregulation of multiple genes specifically involved in the biosynthesis and transport of sulfur-containing amino acids, cysteine and methionine, in the 2DG treated cells at both early and late time points of pseudohyphal development. This transcriptional downregulation was further validated at the protein level for key proteins involved in the sulfur assimilation pathway (Met4, Met32, Met16, Met10, Cys4 and Cys3), clearly demonstrating the dependence of sulfur metabolism on active glycolysis during fungal morphogenesis. This unexpected link between central carbon metabolism and sulfur metabolism is not restricted to conditions that induce fungal morphogenesis *i.e.* in surface-attached colonies grown in nitrogen-limiting conditions since even in liquid cultures that have limiting levels of nitrogen, wherein *S. cerevisiae* cells do not undergo pseudohyphal differentiation (Gancedo, 2001), perturbation of glycolysis with 2DG results in significantly reduced expression of proteins involved in the sulfur assimilation pathway (Met32, Met16, Met10 and Cys3).

Given that multiple genes that encode for proteins involved in *de novo* biosynthesis of sulfur-containing amino acids were downregulated in the presence of 2DG, which strongly inhibits fungal morphogenesis, we wanted to explore the possibility that perturbation of sulfur metabolism is causal for the attenuation of fungal morphogenesis in the presence of 2DG. We tested the functional relevance of this glycolysis-dependent regulation of sulfur metabolism in fungal morphogenesis directly through exogenous supplementation of sulfur sources. The functional significance of glycolysis-dependent regulation of sulfur metabolism was demonstrated through our sulfur add-back experiments wherein,

exogenous supplementation with cysteine specifically rescued the pseudohyphal differentiation defect exhibited by *S. cerevisiae* in the presence of 2DG. Interestingly, methionine alone was unable to rescue the pseudohyphal differentiation defect, in the presence of 2DG even at various different concentrations (50μM, 100μM, 200μM and 500μM). Furthermore, the pseudohyphal differentiation defects observed in the *ΔΔpfk1* and *ΔΔadh1* strains were completely rescued by the addition of cysteine or methionine. These findings strongly implicate that *de novo* biosynthesis of sulfur-containing amino acids is a critical downstream effector of glycolytic activity in promoting pseudohyphal differentiation under nitrogen limitation. To directly assess the role of sulfur metabolism in fungal morphogenesis, we generated and characterized the *met32* deletion strain. This particular strain was critical for our investigation because, unlike most other deletions involving genes that encode for proteins involved in the *de novo* biosynthesis of sulfur-containing amino acids, *met32* deletion does not result in auxotrophy for methionine or cysteine. This unique characteristic is attributed to the functional redundancy provided by its paralog, *met31* (Blaiseau et al., 1997). The deletion of *met32* resulted in substantial defects in pseudohyphal differentiation under nitrogen-limiting conditions, directly implicating the role of sulfur metabolism in regulating fungal morphogenesis. Our sulfur add-back experiments demonstrated that cysteine or methionine rescued the morphogenetic defects exhibited by the *met32* knockout strain, further solidifying the direct involvement of sulfur metabolism in this morphogenetic switching process. How active sulfur metabolism contributes towards fungal morphogenesis is not yet understood but given its critical requirement during this phenomenon, it would be an important question to explore and will further our overall understanding of this important biological phenomenon.

It is interesting to note that the expression of Met4, the principal transcriptional regulator of the *de novo* biosynthesis of sulfur-containing amino acids in *S. cerevisiae* along with Met32 one of its cognate DNA-binding cofactors (Blaiseau et al., 1997), are significantly downregulated when glycolysis is perturbed. Given the obligate requirement of Met4 interaction with DNA-binding proteins such as Met28, Met32, or Met31, to elicit transcriptional activation of the genes involved in the *de novo* biosynthesis of sulfur-containing amino acids (Blaiseau and Thomas, 1998), the observed downregulation in both Met4 and Met32 levels likely compromises the overall biosynthesis of sulfur-containing amino acids. This concurrent downregulation could explain the attenuated expression of downstream genes involved in the synthesis of methionine and cysteine. This suggests a novel regulatory mechanism wherein the expression of Met4/Met32 is coupled to glycolytic activity, under nitrogen-limiting conditions. Given that sulfur metabolism is coupled to glycolysis in *C. albicans* as well and contributes towards fungal morphogenesis, it is likely that this conserved regulatory axis might be critical for fungal morphogenesis in a broad range of fungal species.

Interestingly, Met4 regulation is directly dependent on Met30 (Rouillon et al., 2000). Met30 functions as a molecular switch for Met4, the master regulator of the *Met* gene network. Under sulfur replete conditions, Met30 ensures that Met4 remains inactive through ubiquitination and proteasomal degradation. Conversely, a reduction in sulfur availability diminishes Met30 activity, thereby de-repressing Met4 and allowing it to induce the expression of genes necessary for sulfur amino acid biosynthesis (Rouillon et al., 2000; Smothers et al., 2000; Thomas and Surdin-Kerjan, 1997). Given this regulatory mechanism, we investigated the expression of proteins involved in the sulfur assimilation pathway (Met4, Met32, Met16 and Cys3), in a viable *Δmet30* deletion strain, under

796 conditions where glycolysis was perturbed using 2DG. We observed no difference in protein
797 levels of Met4, Met32, Met16 and Cys3, between 2DG treated and untreated cells. This
798 indicates that, in the heterozygous deletion strain of *met30* (*Δmet30*), Met4 is not
799 degraded even when glycolysis is perturbed, supporting the hypothesis that perturbing
800 active glycolysis with inhibitors like 2DG increases Met30 activity, which in turn leads to
801 the increased degradation of Met4, which would then negatively affect *Met* gene
802 transcription subsequently attenuating pseudohyphal differentiation. However, a
803 surprising finding emerged when we examined Met30 levels in the presence of 2DG. There
804 was no increase in the levels of Met30 in 2DG treated cells compared to untreated cells.
805 This suggests that glycolysis influences Met30 activity through a post-translational
806 mechanism, rather than by altering its protein abundance. Studies have shown that under
807 cadmium stress, Met4 activity is upregulated by reducing the activity of Met30 through
808 post-translational events, specifically by inducing the dissociation of Met30 from the core
809 SCF complex without affecting Met30 protein levels (Yen et al., 2005). This well-
810 established paradigm provides a compelling framework for our observation, suggesting
811 that active glycolytic flux, similar to cadmium stress, might rapidly modulate the activity
812 of Met30 by decreasing its association with the SCF complex to control Met4 activity, rather
813 than through changes in protein synthesis or degradation. Future studies will be needed
814 to delineate the precise post-translational modifications or regulatory interactions that
815 modulate Met30 activity in response to glycolytic flux.
816
817 Intriguingly, our work extended these findings to the pathogenic fungus *C. albicans*,
818 revealing a conserved role for glycolysis-mediated sulfur metabolism in hyphal
819 differentiation, a key virulence attribute in this species (Gow et al., 2012; Moyes et al.,
820 2016; Wilson et al., 2016). Similar to our observations in *S. cerevisiae*,
821 *C. albicans* exhibited glycolysis-dependent hyphal formation under nitrogen limitation,
822 which was inhibited by 2DG. Consistent with our findings in *S. cerevisiae*, RT-qPCR
823 analysis revealed a significant downregulation of genes involved in *de novo* biosynthesis
824 of sulfur-containing amino acids (*met32*, *met3, met5* (*ecm17*), *met10* and *met17*
825 (*met15*)) upon 2DG treatment in *C. albicans*. Importantly, exogenous addition of cysteine
826 and methionine rescued the hyphal differentiation defects caused by 2DG in *C. albicans*,
827 suggesting a conserved link between glycolysis and sulfur metabolism in regulating
828 morphogenesis. Furthermore, a *C. albicans* strain lacking *pfk1,* displayed attenuated
829 hyphal differentiation and significant downregulation of genes involved in *de novo*
830 biosynthesis of sulfur-containing amino acids (*met32*, *met3, met5*
831 (*ecm17*), *met10*, *met17* (*met15*)), which was rescued by cysteine and methionine
832 supplementation, mirroring our observations in *S. cerevisiae*. These results clearly
833 demonstrate that *de novo* biosynthesis of sulfur-containing amino acids is a critical
834 downstream effector of glycolytic activity in promoting hyphal differentiation under
835 nitrogen-limiting conditions, in *C. albicans* as well. Given that central carbon metabolic
836 pathways like glycolysis and sulfur assimilation pathway are broadly conserved metabolic
837 processes across a plethora of fungal species, it is possible that this novel regulatory axis
838 might play a crucial role in modulating fungal morphogenesis in multiple fungal species
839 and further studies are warranted to explore this. Finally, given the established link
840 between hyphal differentiation and *C. albicans* virulence, we explored the impact of
841 glycolytic perturbation on the pathogenicity of this fungus. Interestingly, RT-qPCR analysis
842 revealed a significant downregulation of genes involved in hyphal differentiation and
843 virulence (*als3, ece1, hwp1, hyr1, ihd1, rbt1* and *sap6*) upon 2DG treatment and in the
844 *ΔΔpfk1* strain. Interestingly, deletions of sugar kinases or transcription factors regulating
845 the expression of glycolysis genes or *adh1* in *C. albicans* leads to filamentation defects and

846 downregulation of filamentation/virulence-specific genes (Askew et al., 2009; Laurian et
847 al., 2019; Song et al., 2019). Our data, showing transcriptional downregulation of hyphal
848 differentiation and virulence genes following glycolytic perturbation *via* the deletion of
849 *pfk1*, strongly corroborate these previous findings. This collectively positions glycolysis as
850 a central metabolic nexus, rather than merely a catabolic process, profoundly influencing
851 the pathogenic ability of *C. albicans* by intricately linking cellular metabolism,
852 morphogenetic transitions, and the expression of its virulence factors. Furthermore,
853 the *ΔΔpfk1* strain displayed significantly reduced survival within *murine*
854 macrophages and attenuated virulence in a *murine* model of systemic candidiasis, as
855 evidenced by increased host survival, lower kidney fungal burden, and reduced tissue
856 colonization. Remarkably, exogenous sulfur supplementation (N-acetyl cysteine (NAC)) to
857 mice rescued the attenuated virulence exhibited by *ΔΔpfk1*. Specifically, mice receiving
858 NAC-containing distilled water and infected with *ΔΔpfk1* showed significantly reduced
859 survival and increased tissue colonization compared to those given normal distilled water.
860 These findings underscore the critical role of glycolysis, and by extension, glycolysis-
861 dependent sulfur metabolism, in the virulence of *C. albicans*.
862
863 In conclusion, our study unveils a conserved metabolic network that orchestrates fungal
864 morphogenesis in response to nutrient availability. We demonstrate that active glycolysis,
865 fueled by fermentable carbon sources in a cAMP-PKA independent manner, plays a crucial
866 role in regulating the *de novo* biosynthesis of sulfur-containing amino acids in Met30-
867 dependent manner, which in turn are essential for the morphological transitions in both
868 *S. cerevisiae* and *C. albicans* (Fig. 6). The attenuation of *C. albicans* virulence upon
869 disruption of this pathway highlights the potential of targeting specific fungal metabolic
870 networks as a novel antifungal strategy. Future research in our laboratory will focus on
871 elucidating the precise molecular mechanisms by which glycolytic intermediates or
872 downstream signals regulate the expression of sulfur metabolism pathway and how sulfur-
873 containing amino acids contribute to the cellular processes underlying fungal
874 morphogenesis.
875

876 ## Materials and Methods

877
878 **Yeast Strains:**
879 The prototrophic diploid strains, ∑1278b or CEN.PK were used in all the experiments
880 involving *S. cerevisiae*. The prototrophic diploid strain, SC5314 was exclusively used in all
881 the experiments involving *C. albicans*. The yeast strains used in this study are listed in
882 Suppl.Table 1.
883
884 **Generation of *S. cerevisiae* Gene Knockout and Epitope-tagged Strains:**
885 A standard PCR-based technique was used to amplify resistance cassettes (G418, HygB,
886 or NAT) with flanking sequences in order to carry out gene deletions. The target gene was
887 then replaced by homologous recombination using the lithium acetate-based
888 transformation (Schiestl and Gietz, 1989). Similarly, C-terminal epitope-tagged yeast
889 strains were generated using a PCR-based technique. This involved amplifying resistance
890 cassettes, flanked by sequences homologous to the C-terminal region of the target gene,
891 along with the desired epitope tags. The targeted gene was then tagged at its C-terminus
892 through homologous recombination, using the lithium acetate-based transformation
893 method. Primers used for these experiments are listed in Suppl.Table 2.
894

895 **Generation of *C. albicans* Gene Knockout Strains:**
896 The *C. albicans* strains used in this study are listed in Suppl.Table 1. The previously
897 established SAT1-flipper method was used with some modifications, for the deletion of the
898 desired genes (Reuß et al., 2004). To generate the *pfk1* deletion (*ΔΔpfk1*) strain, a DNA
899 fragment carrying the flanking regions of *pfk1* (100 bps homology) and the *SAT1*-flipper
900 cassette was transformed into *C. albicans* wild-type SC5314, using electroporation.
901 Transformants were selected based on their nourseothricin resistance. PCR confirmation
902 was used to validate the transformants. The *SAT1*-flipper cassette was then excised from
903 the *pfk1* locus by growing the cells in YPM medium (10g/l yeast extract, 20g/l peptone,
904 and 2% (w/v) maltose) to induce expression of the *MAL2* promoter-regulated
905 recombinase. To knock out the second allele of *pfk1*, the heterozygous *pfk1* deletion
906 mutants (*Δpfk1/PFK1)* were used for the transformation wherein the DNA fragment
907 carrying the flanking regions of *pfk1* (100 bps homology) and the *SAT1*-flipper cassette
908 was transformed into *C. albicans Δpfk1/PFK1* SC5314. Transformants were selected based
909 on their nourseothricin resistance. PCR confirmation was used to validate the
910 transformants. Primers used to generate or confirm the deletion strains are listed in
911 Suppl.Table 2.
912
913 **Media and Growth Conditions:**
914 YPD broth containing 10g/l yeast extract, 20g/l peptone and 2% (w/v) glucose was used
915 for the overnight growth of the cultures. Nitrogen-limiting medium containing 1.7g/l yeast
916 nitrogen base without amino acids or ammonium sulfate, 2% (w/v) glucose (SLAD) or
917 various different fermentable or non-fermentable carbon sources, 50μM ammonium
918 sulfate and 2% (w/v) agar which was extensively washed, to remove excess nitrogen
919 (Gimeno et al., 1992) was used for all experiments involving pseudohyphal or hyphal
920 differentiation. Overnight cultures of various strains were grown in YPD broth and
921 incubated at 30 °C with continuous shaking at 200 rotations per minute (RPM). Reagents
922 and tools used in this study are mentioned in Suppl.Table 3.
923
924 **Pseudohyphal Differentiation Assay:**
925 To induce pseudohyphal differentiation in *S. cerevisiae,* overnight cultures of various
926 strains (listed in Suppl.Table 1) were spotted on nitrogen-limiting medium (SLA)
927 containing 2% glucose (SLAD). In order to check the effect of glycolysis inhibitors, 0.05%
928 concentration of 2-Deoxy-D-Glucose (2DG) and 0.2% concentration of sodium citrate
929 (NaCi), on pseudohyphal differentiation, wild-type was spotted on SLAD containing sub-
930 inhibitory concentrations of 2DG (0.05%) or NaCi (0.2%). Plates were incubated for 10
931 days at 30 °C (Chandarlapaty and Errede, 1998; González et al., 2017). After 10 days,
932 imaging was done using Olympus MVX10 stereo microscope. Cells from colonies were
933 isolated and single cells were imaged using Zeiss Apotome microscope and the percentage
934 of pseudohyphal cells was calculated using ImageJ. Cells with a length/width ratio of 2 or
935 more were considered as pseudohyphal cells as described previously (Schröder et al.,
936 2000). Statistical analysis was done using unpaired t-test or one-way ANOVA test. Error
937 bars represent SEM. All the experiments were performed independently, thrice.
938
939 **Hyphal Differentiation Assay:**
940 To induce hyphal differentiation in *C. albicans,* overnight cultures of each strain (listed in
941 Suppl.Table 1) were spotted on nitrogen-limiting medium (SLAD). To check the effect of
942 glycolysis inhibitor, 2-Deoxy-D-Glucose (2DG) on hyphal differentiation, wild-type was
943 spotted on SLAD containing sub-inhibitory concentration of 2DG (0.2%). All the plates
944 were incubated for 7 days at 37 °C (Sánchez-Martínez and Pérez-Martín, 2002; Song et

al., 2019). After 7 days, cells from colonies were isolated and single cells were imaged using Zeiss Apotome microscope and percentage of hyphal cells was calculated using ImageJ. Cells with a length/width ratio of 4.5 or more were considered as hyphal cells as described previously (Su et al., 2018). Statistical analysis was done using unpaired t-test. Error bars represent SEM. All the experiments were performed independently, thrice.

Growth Curves:

Growth curve analysis in the presence of glycolysis inhibitors (2DG or NaCi) was performed as follows. Overnight grown cultures of wild-type strains (∑1278b or CEN.PK or SC5314) were diluted to OD_{600}=0.01 in fresh SLAD medium with and without 2DG or NaCi and allowed to grow at 30 °C for 24 hours. OD_{600} was recorded at 3-h intervals. Growth curve analysis using various deletion strains were performed as follows. Overnight grown cultures of various deletion strains along with wild-type strains (∑1278b or CEN.PK or SC5314) were diluted to OD_{600}=0.01 in fresh SLAD and allowed to grow at 30 °C for 24 hours. OD_{600} was recorded at 3-h intervals. Graphs were prepared using GraphPad Prism. Error bars represent SEM. All the experiments were performed independently, thrice.

cAMP Add-back Assays:

In order to perform cAMP add-back assays, overnight cultures of wild-type ∑1278b and various deletion strains of *S. cerevisiae* (listed in Suppl.Table 1) were spotted on SLAD or SLAD containing sub-inhibitory concentration of 2DG or NaCi, in the presence and absence of cAMP (1mM) (Lorenz, 1997). Plates were incubated for 10 days at 30 °C to induce pseudohyphal differentiation in *S. cerevisiae*. After 10 days, imaging was done using Olympus MVX10 stereo microscope. All the experiments were performed independently, thrice.

Sulfur Add-back Assays:

In order to perform sulfur add-back assays, overnight cultures of various strains of *S. cerevisiae* or *C. albicans* (listed in Suppl.Table 1) were spotted on SLAD or SLAD containing sub-inhibitory concentration of 2DG, in the presence and absence of sulfur-containing compounds including cysteine, methionine. Plates were incubated for 10 days at 30 °C to induce pseudohyphal differentiation in *S. cerevisiae*. After 10 days, imaging was done using Olympus MVX10 stereo microscope. Cells from colonies were isolated and single cells were imaged using Zeiss Apotome microscope and percentage of pseudohyphal cells were calculated using ImageJ. For hyphal differentiation assays in *C. albicans*, plates were incubated for 7 days at 37 °C. After 7 days, cells from colonies were isolated and single cells were imaged using Zeiss Apotome microscope and percentage of hyphal cells were calculated using ImageJ. Statistical analysis was done using unpaired t-test or one-way ANOVA test. Error bars represent SEM. All the experiments were performed independently, thrice.

Whole genome sequencing:

Sample Collection. Strains of *S. cerevisiae* (*ΔΔpfk1* or *ΔΔadh1* along with wild-type strain ∑1278b) or *C. albicans* (*ΔΔpfk1* along with wild-type strain SC5314) were grown in YPD medium at 30 °C for overnight.

Genomic DNA Extraction. Genomic DNA from the samples was extracted using phenol-chloroform method. Following RNAse treatment to eliminate any contaminating RNA from the sample, the extracted DNA was submitted to the CCMB next-generation sequencing facility for whole genome sequencing.

995 **Whole genome sequencing Analysis.** Raw sequencing reads were obtained in FASTQ
996 format. The reference genome and annotation files for the *S. cerevisiae* strain ∑1278b
997 were downloaded from the Saccharomyces Genome Database (SGD) and reference
998 genome and annotation files for the *C, albicans* strain SC5314 were downloaded from the
999 NCBI (National Center for Biotechnology Information). Quality assessment of the raw
1000 reads was performed using FastQC (version 0.12.1). Adapter sequences were trimmed
1001 using Cutadapt (version 4.6). The reference genome was indexed with Hisat2 (version
1002 2.2.1), and Samtools (version 1.20) was used to filter out multi-mapped reads and convert
1003 SAM files to BAM format. Visualisation of reads was done using IGV software (version
1004 2.16.2).
1005
1006 **RNA-Sequencing:**
1007 **Sample Collection.** Overnight culture of *S. cereviae* wild-type ∑1278b was spotted on
1008 nitrogen-limiting media containing 2% (w/v) glucose (SLAD) with and without sub-
1009 inhibitory concentration of 2-Deoxy-D-Glucose (2DG). The plates were incubated at 30 °C
1010 and colonies were isolated on day 5 (D-5) and day 10 (D-10).
1011
1012 **RNA-Extraction.** Total RNA from the sample was extracted using the protocol mentioned
1013 in the Ribopure RNA purification kit (yeast) (cat. #AM1926). Following a DNAse treatment
1014 to eliminate any genomic DNA from the sample, the extracted RNA was submitted to the
1015 CCMB next-generation sequencing facility for RNA-Seqencing. The NovaSeq 6000
1016 equipment was used to sequence transcriptomes.
1017
1018 **RNA-Sequencing Analysis.** Raw sequencing reads were obtained in FASTQ format. The
1019 reference genome and annotation files for the *S. cerevisiae* strain ∑1278b were
1020 downloaded from the Saccharomyces Genome Database (SGD). Quality assessment of the
1021 raw reads was performed using FastQC (version 0.12.1). Adapter sequences were trimmed
1022 using Cutadapt (version 4.6). The reference genome was indexed with Hisat2 (version
1023 2.2.1), and Samtools (version 1.20) was used to filter out multi-mapped reads and convert
1024 SAM files to BAM format. Read counting for uniquely mapped reads was done with
1025 FeatureCounts, using gene annotation data from the reference *S. cerevisiae* ∑1278b
1026 genome. Normalization and differential gene expression analysis were performed using
1027 R (version 4.3.2). Genes with a $\log_2$ fold change of ≥1 were considered to be upregulated,
1028 indicating at least a doubling in expression under the given condition, while those with a
1029 $\log_2$ fold change of ≤ -1 were considered to be downregulated.
1030
1031 **Protein Isolation:**
1032 For Western blotting experiments, in order to isolate proteins from liquid cultures,
1033 overnight yeast cultures were back-diluted in 10 ml of liquid SLAD in the presence and
1034 absence of 2-Deoxy-D-Glucose (2DG). The yeast cells were grown till an OD_{600} of ~1 and
1035 cells were harvested by centrifugation at 3000 rpm for 10 minutes at room temperature
1036 (RT). To isolate proteins from colonies, overnight cultures of pertinent strains were spotted
1037 on SLAD with and without sub-inhibitory concentration of 2-Deoxy-D-Glucose (2DG)
1038 (0.05%) and colonies were isolated and resuspended in 1ml of 1X PBS (Phosphate Buffered
1039 Saline) after 5 days (D-5). Cells were harvested by centrifugation at 14000 rpm for 10
1040 minutes at room temperature. Pelleted cells (from liquid cultures and colonies) were
1041 resuspended in 300µl of ice cold 10% (w/v) TCA solution and disrupted using bead-beating
1042 by addition of 150µl of glass beads at 4°C. Supernatant was transferred to another tube.
1043 Next, proteins were pelleted by centrifugation at 14,000 rpm for 10 minutes at 4°C and
1044 supernatant was discarded. Each pellet was resuspended in 400µl of SDS/glycerol buffer

1045 (7.3% (w/v) SDS, 29% (v/v) glycerol and 83.3mM tris-base) and boiled at 95°C for 10
1046 minutes with occasional vortexing followed by centrifugation at 14,000 rpm for 10 minutes
1047 at room temperature. Supernatant was transferred to a fresh tube and used for protein
1048 estimation using BCA protein estimation kit (cat. #23227). Finally, all samples were diluted
1049 in SDS-PAGE loading buffer (100mM Tris-Cl, 4% (w/v) SDS, 0.02% (w/v) bromophenol
1050 blue, 20% (w/v), glycerol and 7.5% (v/v) β-mercaptoethanol) and heated for 5 minutes
1051 at 90 °C.
1052
1053 **Immunodetection:**
1054 Protein samples were separated using SDS-PAGE on polyacrylamide gels and transferred
1055 to PVDF membranes with a Mini Trans-Blot Cell module (Bio-Rad). The membranes were
1056 blocked for 1 hour at room temperature with 5% (w/v) non-fat dry milk in 1X TBST buffer
1057 (20 mM Tris-Base, pH 7.6, 150 mM NaCl, 0.1% (v/v) Tween-20) with gentle orbital
1058 shaking. After blocking, the membranes were incubated overnight at 4°C with primary
1059 antibodies (1:2000 dilution) in 1X TBST buffer containing 5% (w/v) non-fat dry milk.
1060 Following this, the membranes were washed three times for 10 minutes in 1X TBST and
1061 then incubated for 1 hour at room temperature with HRP-conjugated secondary antibodies
1062 (1:4000 dilution) in 1X TBST with 5% (w/v) non-fat dry milk. After three additional washes
1063 in 1X TBST, chemiluminescent substrate was added and bands were detected using the
1064 SuperSignal West chemiluminescent substrate (cat. #34579, cat. #34094) and visualized
1065 using the Bio-Rad ChemiDoc™ MP imaging system. All the experiments were performed
1066 independently, thrice.
1067
1068 **Antibodies:**
1069 HA-Tag (C29F4) Rabbit mAb (cat. #3724), β-actin (8H10D10) Mouse mAb (cat. #3700),
1070 Goat anti-Rabbit IgG-HRP conjugate (cat. #7074) and Horse anti-Mouse IgG-HRP
1071 conjugate (cat. #7076) were purchased from Cell Signaling Technology. Pgk1 Mouse mAb
1072 (cat. #sc-130335) was purchased from Santa Cruz Biotechnology.
1073
1074 **Densitometric Analysis:**
1075 Raw images of Western blots were analysed using ImageJ to normalize target protein
1076 expression with the expression of housekeeping proteins including PGK1 and β-actin in
1077 order to make densitometric graphs. Statistical analysis was done using unpaired t-test,
1078 with error bars representing SEM. All the experiments were performed independently,
1079 thrice.
1080
1081 **Quantitative Real Time Polymerase Chain Reaction (RT-qPCR) Assay:**
1082 Overnight cultures of *C. albicans* wild-type SC5314 was spotted on SLAD with and without
1083 sub-inhibitory concentration of 2-Deoxy-D-Glucose (2DG) (0.2%) or *C. albicans ΔΔpfk1*
1084 strain along with wild-type SC5314 was spotted on SLAD and plates were incubated at
1085 37 °C for 4 days. After 4 days, colonies were isolated and total RNA was extracted using
1086 the protocol mentioned in the Ribopure RNA purification kit, yeast (cat. #AM1926). cDNA
1087 synthesis was carried out using PrimeScript cDNA synthesis kit (cat. #6110A). Primers
1088 used for RT-qPCR were designed using PrimeQuest tool of Integrated DNA Technologies
1089 (IDT). RT-qPCR was performed using iTaq Universal SYBR green mastermix (cat.
1090 #1725121). Actin was used as housekeeping gene for normalization. The results were
1091 analysed using the $2^{-\Delta\Delta CT}$ method (Winer et al., 1999) and statistical analysis was done
1092 using one-way ANOVA test, with error bars representing SEM. All the experiments were
1093 performed independently, thrice. Primers used in the RT-qPCR experiments are mentioned
1094 in Suppl.Table 2.

1095 ***In vitro* Microbial Survival Assay:**
1096 *In vitro* microbial survival assay in macrophages was conducted as described in previous
1097 studies with some modifications (Netea et al., 2002; Pradhan et al., 2016). *RAW 264.7*
1098 macrophages (1×10^6 cells) were cultured in six-well plates with DMEM supplemented with
1099 10% FBS. After 16 hours of incubation, the cells were treated with *C. albicans* wild-type
1100 SC5314 or *ΔΔpfk1* at a multiplicity of infection (MOI) of 10, for 1 hour in antibiotic-free
1101 DMEM containing 10% FBS. The media was then removed, and the cells were washed six
1102 times with 1X PBS to eliminate any free, non-phagocytosed fungal cells. Next, the cells
1103 were lysed with 350 µl of lysis buffer containing 0.025% SDS in 1X PBS. The lysate volume
1104 was adjusted to 1 ml with 1X PBS, and a 100 µl undiluted aliquot was plated on YPD agar
1105 plate. Serial dilutions of the lysate were also plated on YPD agar plates. These plates were
1106 incubated overnight at 37 °C. The following day, colony forming units (CFU) were counted
1107 and plotted. The percentage of survival was calculated as the number of CFU in the
1108 presence of macrophages divided by the number of CFU in the absence of macrophages.
1109 Statistical analysis was done using unpaired t-test, with error bars representing SEM. All
1110 the experiments were performed independently, thrice.
1111
1112 ***In vivo Murine* Model of Systemic Candidiasis:**
1113 *In vivo* infection experiments were performed as previously described (Majer et al., 2012).
1114 Briefly, *C. albicans* wild-type SC5314 and *ΔΔpfk1* were grown overnight in YPD medium
1115 at 30 °C. The overnight cultures were back-diluted in 10 ml of YPD liquid medium and
1116 allowed to grow till and OD of ~0.6, then washed and resuspended (1×10^7 CFU) in 1X
1117 PBS. C57BL/6 wild-type mice, aged 6 to 8 weeks, were injected intravenously *via* lateral
1118 tail vein with *C. albicans* wild-type SC5314 (1×10^7 CFU) or *ΔΔpfk1* (1×10^7 CFU). After
1119 infection, mice were monitored for survival and daily for signs of morbidity and mortality
1120 were recorded over a period of 21 days. Survival data were analysed using the Log-rank
1121 Mantel-Cox test In order to perform *in vivo* sulfur supplementation, N-acetyl cysteine
1122 (NAC) was dissolved in distilled water at a concentration of 6mg/ml and administrated
1123 orally to mice before 72 hours of *C. albicans* infection. Normal distilled water administration
1124 to mice was used as control. After 72 hours of NAC administration, C57BL/6 wild-type
1125 mice, aged 6 to 8 weeks, were infected with SC5314 (1×10^7 CFU) or *ΔΔpfk1* strain ($1 \times$
1126 10^7 CFU), intravenously *via* lateral tail vein injection. After infection, mice were monitored
1127 for survival and daily for signs of morbidity and mortality were recorded over a period of
1128 21 days. Survival data were analysed using the Log-rank Mantel-Cox test.
1129
1130 **Determination of Fungal Burden:**
1131 To assess fungal burden, mice injected with *C. albicans* wild-type SC5314 or *ΔΔpfk1* were
1132 sacrificed at ~2 days and kidneys were harvested from infected mice. Kidneys were
1133 weighed and then homogenized using a sterilized and PBS-washed Dounce homogenizer
1134 (cat. #D8938). Kidney suspensions were then diluted in 1 ml of 1X PBS and serially diluted.
1135 Then 100µl of dilutions was plated on YPD agar plates and allowed to grow at 37 °C. Colony
1136 forming units (CFU) were calculated by the following formula: (number of colonies ×
1137 dilution factor × 10)/organ weight in grams (g). Statistical analysis was done using
1138 unpaired t-test. Error bars represent SEM. All the experiments were performed
1139 independently, thrice.
1140
1141 **Histopathology:**
1142 For histopathological examination, kidneys were collected and fixed in 10% neutral
1143 buffered formalin for about two weeks. After fixation, the kidneys were processed,
1144 embedded in paraffin, and sectioned to 4 µm thickness. The tissue sections were then

stained using the GMS stain (Grocott Methenamine Silver stain) and the protocol mentioned in the GMS staining kit manual (cat. #AB287884) was followed. All the experiments were performed independently, thrice.

Illustrations:

Figure illustrations were created using Biorender (https://app.biorender.com).

Animal Ethics Statement:

All animal experiments in this manuscript were reviewed and approved by the Institutional Animal Ethics Committee (IAEC) of CSIR-Centre for Cellular and Molecular Biology (Approval number: 52/2024-C).

Data Availability:

All relevant data are within the paper and its supporting information files, except for RNA-Seq data. RNA-Seq data are deposited in NCBI's SRA database and are accessible through BioProject accession number PRJNA1263201. (https://www.ncbi.nlm.nih.gov/bioproject/PRJNA1263201)

Acknowledgements

We gratefully acknowledge the invaluable support and resources offered by CSIR-Centre for Cellular and Molecular Biology (CCMB) central facilities including Advanced Microscopy and Imaging facility (AMIF), Next Generation Sequencing (NGS) facility and Animal House facility. We acknowledge help from T. Avinash Raj (CSIR- CCMB) for preparation of samples for histological analysis. DS thanks University Grants Commission (UGC), India for their research fellowship. SV acknowledges funding from Indian Council of Medical Research (ICMR) (IIRPSG-2024-01-02717), India; Anusandhan National Research Foundation (ANRF) (SRG/2023/000470), India; Council of Scientific & Industrial Research (CSIR) (FTT070505), India; and DBT-Wellcome Trust India Alliance (IA/E/16/1/502996), India.

Author Contributions

Dhrumi Shah: Conceptualization; Investigation; Formal analysis; Visualization; Writing-original draft. **Nikita Rewatkar:** Investigation. **Adishree M:** Investigation. **Siddhi Gupta:** Investigation. **Sudharsan Mathivathanan:** Investigation. **Sayantani Biswas:** Investigation. **Sriram Varahan:** Conceptualization; Supervision; Funding acquisition; Investigation; Formal analysis; Visualization; Writing-original draft; Writing-review and editing.

Conflict of Interest

The authors declare that they have no conflict of interests.

References

1. Askew, C., Sellam, A., Epp, E., Hogues, H., Mullick, A., Nantel, A., & Whiteway, M. (2009). Transcriptional regulation of carbohydrate metabolism in the human pathogen Candida albicans. *PLoS pathogens*, *5*(10), e1000612. https://doi.org/10.1371/journal.ppat.1000612
2. Bailey, D. A., Feldmann, P. J., Bovey, M., Gow, N. A., & Brown, A. J. (1996). The Candida albicans HYR1 gene, which is activated in response to hyphal development, belongs to a gene family encoding yeast cell wall proteins. Journal of bacteriology, 178(18), 5353–5360. https://doi.org/10.1128/jb.178.18.5353-5360.1996
3. Barford JP, Hall RJ. 1979. An examination of the crabtree effect in Saccharomyces cerevisiae: The role of respiratory adaptation. J Gen Microbiol. doi:10.1099/00221287-114-2-267
4. Bennetzen, J. L., & Hall, B. D. (1982). The primary structure of the Saccharomyces cerevisiae gene for alcohol dehydrogenase. The Journal of biological chemistry, 257(6), 3018–3025.
5. Biswas, S., Van Dijck, P., & Datta, A. (2007). Environmental sensing and signal transduction pathways regulating morphopathogenic determinants of Candida albicans. Microbiology and molecular biology reviews : MMBR, 71(2), 348–376. https://doi.org/10.1128/MMBR.00009-06
6. Blaiseau, P. L., Isnard, A. D., Surdin-Kerjan, Y., & Thomas, D. (1997). Met31p and Met32p, two related zinc finger proteins, are involved in transcriptional regulation of yeast sulfur amino acid metabolism. Molecular and cellular biology, 17(7), 3640–3648. https://doi.org/10.1128/MCB.17.7.3640
7. Blaiseau, P. L., & Thomas, D. (1998). Multiple transcriptional activation complexes tether the yeast activator Met4 to DNA. The EMBO journal, 17(21), 6327–6336. https://doi.org/10.1093/emboj/17.21.6327
8. Broach J. R. (2012). Nutritional control of growth and development in yeast. Genetics, 192(1), 73–105. https://doi.org/10.1534/genetics.111.135731
9. Chandarlapaty, S., & Errede, B. (1998). Ash1, a daughter cell-specific protein, is required for pseudohyphal growth of Saccharomyces cerevisiae. Molecular and cellular biology, 18(5), 2884–2891. https://doi.org/10.1128/MCB.18.5.2884
10. Chebaro, Y., Lorenz, M., Fa, A., Zheng, R., & Gustin, M. (2017). Adaptation of Candida albicans to Reactive Sulfur Species. Genetics, 206(1), 151–162. https://doi.org/10.1534/genetics.116.199679
11. Christensen, M. (1989). A View of Fungal Ecology. Mycologia, 81(1), 1–19. https://doi.org/10.1080/00275514.1989.12025620
12. Francis B. Cramer, Gladys E. Woodward, 2-Desoxy-D-glucose as an antagonist of glucose in yeast fermentation, Journal of the Franklin Institute, Volume 253, Issue 4, 1952, Pages 354-360, ISSN 0016-0032, https://doi.org/10.1016/0016-0032(52)90852-1
13. Csank, C., Schröppel, K., Leberer, E., Harcus, D., Mohamed, O., Meloche, S., Thomas, D. Y., & Whiteway, M. (1998). Roles of the Candida albicans mitogen-activated protein kinase homolog, Cek1p, in hyphal development and systemic candidiasis. Infection and immunity, 66(6), 2713–2721. https://doi.org/10.1128/IAI.66.6.2713-2721.1998
14. De Deken R. H. (1966). The Crabtree effect: a regulatory system in yeast. Journal of general microbiology, 44(2), 149–156. https://doi.org/10.1099/00221287-44-2-149
15. Deorukhkar SC, Roushani S (2017) Virulence Traits Contributing to Pathogenicity of Candida Species. J Microbiol Exp 5(1): 00140. DOI: 10.15406/jmen.2017.05.00140
16. Dickinson, J. R., Salgado, L. E., & Hewlins, M. J. (2003). The catabolism of amino acids to long chain and complex alcohols in Saccharomyces cerevisiae. The Journal of biological chemistry, 278(10), 8028–8034. https://doi.org/10.1074/jbc.M211914200
17. Dikicioglu, D., Karabekmez, E., Rash, B., Pir, P., Kirdar, B., & Oliver, S. G. (2011). How yeast re-programmes its transcriptional profile in response to different nutrient impulses. BMC systems biology, 5, 148. https://doi.org/10.1186/1752-0509-5-148
18. Christopher Thomas Evans and Colin Ratledge. 1985. Partial purification and properties of pyruvate kinase and its regulatory role during lipid accumulation by the oleaginous yeast Rhodosporidium toruloides CBS 14. Canadian Journal of Microbiology. 31(5): 479-484. https://doi.org/10.1139/m85-089
19. Fleck, C. B., Schöbel, F., & Brock, M. (2011). Nutrient acquisition by pathogenic fungi: nutrient availability, pathway regulation, and differences in substrate utilization.

International journal of medical microbiology : IJMM, 301(5), 400–407. https://doi.org/10.1016/j.ijmm.2011.04.007

20. Foy, J. J., & Bhattacharjee, J. K. (1978). Biosynthesis and regulation of fructose-1,6-bisphosphatase and phosphofructokinase in Saccharomyces cerevisiae grown in the presence of glucose and gluconeogenic carbon sources. Journal of bacteriology, 136(2), 647–656. https://doi.org/10.1128/jb.136.2.647-656.1978
21. Gancedo J. M. (2001). Control of pseudohyphae formation in Saccharomyces cerevisiae. FEMS microbiology reviews, 25(1), 107–123. https://doi.org/10.1111/j.1574-6976.2001.tb00573.x
22. Gimeno, C. J., Ljungdahl, P. O., Styles, C. A., & Fink, G. R. (1992). Unipolar cell divisions in the yeast S. cerevisiae lead to filamentous growth: regulation by starvation and RAS. Cell, 68(6), 1077–1090. https://doi.org/10.1016/0092-8674(92)90079-r
23. González, B., Mas, A., Beltran, G., Cullen, P. J., & Torija, M. J. (2017). Role of Mitochondrial Retrograde Pathway in Regulating Ethanol-Inducible Filamentous Growth in Yeast. Frontiers in physiology, 8, 148. https://doi.org/10.3389/fphys.2017.00148
24. Gow, N. A., Brown, A. J., & Odds, F. C. (2002). Fungal morphogenesis and host invasion. Current opinion in microbiology, 5(4), 366–371. https://doi.org/10.1016/s1369-5274(02)00338-7
25. Gow, N. A., van de Veerdonk, F. L., Brown, A. J., & Netea, M. G. (2011). Candida albicans morphogenesis and host defence: discriminating invasion from colonization. Nature reviews. Microbiology, 10(2), 112–122. https://doi.org/10.1038/nrmicro2711
26. Harashima, T., & Heitman, J. (2002). The Galpha protein Gpa2 controls yeast differentiation by interacting with kelch repeat proteins that mimic Gbeta subunits. Molecular cell, 10(1), 163–173. https://doi.org/10.1016/s1097-2765(02)00569-5
27. Heinisch J. (1986). Construction and physiological characterization of mutants disrupted in the phosphofructokinase genes of Saccharomyces cerevisiae. Current genetics, 11(3), 227–234. https://doi.org/10.1007/BF00420611
28. Hirayama, T., Miyazaki, T., Ito, Y., Wakayama, M., Shibuya, K., Yamashita, K., Takazono, T., Saijo, T., Shimamura, S., Yamamoto, K., Imamura, Y., Izumikawa, K., Yanagihara, K., Kohno, S., & Mukae, H. (2020). Virulence assessment of six major pathogenic Candida species in the mouse model of invasive candidiasis caused by fungal translocation. Scientific reports, 10(1), 3814. https://doi.org/10.1038/s41598-020-60792-y
29. Huang G. (2012). Regulation of phenotypic transitions in the fungal pathogen Candida albicans. Virulence, 3(3), 251–261. https://doi.org/10.4161/viru.20010
30. Jiménez-López, C., & Lorenz, M. C. (2013). Fungal immune evasion in a model host-pathogen interaction: Candida albicans versus macrophages. PLoS pathogens, 9(11), e1003741. https://doi.org/10.1371/journal.ppat.1003741
31. Kaiser, P., Sia, R. A., Bardes, E. G., Lew, D. J., & Reed, S. I. (1998). Cdc34 and the F-box protein Met30 are required for degradation of the Cdk-inhibitory kinase Swe1. Genes & development, 12(16), 2587–2597. https://doi.org/10.1101/gad.12.16.2587
32. Kraakman, L., Lemaire, K., Ma, P., Teunissen, A. W., Donaton, M. C., Van Dijck, P., Winderickx, J., de Winde, J. H., & Thevelein, J. M. (1999). A Saccharomyces cerevisiae G-protein coupled receptor, Gpr1, is specifically required for glucose activation of the cAMP pathway during the transition to growth on glucose. Molecular microbiology, 32(5), 1002–1012. https://doi.org/10.1046/j.1365-2958.1999.01413.x
33. Kumar A. (2021). The Complex Genetic Basis and Multilayered Regulatory Control of Yeast Pseudohyphal Growth. Annual review of genetics, 55, 1–21. https://doi.org/10.1146/annurev-genet-071719-020249
34. Laurian, R., Dementhon, K., Doumèche, B., Soulard, A., Noel, T., Lemaire, M., & Cotton, P. (2019). Hexokinase and Glucokinases Are Essential for Fitness and Virulence in the Pathogenic Yeast Candida albicans. Frontiers in microbiology, 10, 327. https://doi.org/10.3389/fmicb.2019.00327
35. Laxman, S., & Tu, B. P. (2011). Multiple TORC1-associated proteins regulate nitrogen starvation-dependent cellular differentiation in Saccharomyces cerevisiae. PloS one, 6(10), e26081. https://doi.org/10.1371/journal.pone.0026081
36. Li, D. D., Wang, Y., Dai, B. D., Li, X. X., Zhao, L. X., Cao, Y. B., Yan, L., & Jiang, Y. Y. (2013). ECM17-dependent methionine/cysteine biosynthesis contributes to biofilm formation in Candida albicans. Fungal genetics and biology : FG & B, 51, 50–59. https://doi.org/10.1016/j.fgb.2012.11.010

37. Lin, X., Alspaugh, J. A., Liu, H., & Harris, S. (2014). Fungal morphogenesis. Cold Spring Harbor perspectives in medicine, 5(2), a019679. https://doi.org/10.1101/cshperspect.a019679
38. Lionakis, M. S., Lim, J. K., Lee, C. C., & Murphy, P. M. (2011). Organ-specific innate immune responses in a mouse model of invasive candidiasis. Journal of innate immunity, 3(2), 180–199. https://doi.org/10.1159/000321157
39. Liu, Y., & Filler, S. G. (2011). Candida albicans Als3, a multifunctional adhesin and invasin. Eukaryotic cell, 10(2), 168–173. https://doi.org/10.1128/EC.00279-10
40. Lobo, Z., & Maitra, P. K. (1983). Phosphofructokinase mutants of yeast. Biochemistry and genetics. The Journal of biological chemistry, 258(3), 1444–1449.
41. Lorenz, M. C., & Heitman, J. (1997). Yeast pseudohyphal growth is regulated by GPA2, a G protein alpha homolog. The EMBO journal, 16(23), 7008–7018. https://doi.org/10.1093/emboj/16.23.7008
42. Lorenz, M. C., & Heitman, J. (1998). Regulators of pseudohyphal differentiation in Saccharomyces cerevisiae identified through multicopy suppressor analysis in ammonium permease mutant strains. Genetics, 150(4), 1443–1457. https://doi.org/10.1093/genetics/150.4.1443
43. Lorenz, M. C., Pan, X., Harashima, T., Cardenas, M. E., Xue, Y., Hirsch, J. P., & Heitman, J. (2000). The G protein-coupled receptor gpr1 is a nutrient sensor that regulates pseudohyphal differentiation in Saccharomyces cerevisiae. Genetics, 154(2), 609–622. https://doi.org/10.1093/genetics/154.2.609
44. Maidan, M. M., De Rop, L., Serneels, J., Exler, S., Rupp, S., Tournu, H., Thevelein, J. M., & Van Dijck, P. (2005). The G protein-coupled receptor Gpr1 and the Galpha protein Gpa2 act through the cAMP-protein kinase A pathway to induce morphogenesis in Candida albicans. Molecular biology of the cell, 16(4), 1971–1986. https://doi.org/10.1091/mbc.e04-09-0780
45. Majer, O., Bourgeois, C., Zwolanek, F., Lassnig, C., Kerjaschki, D., Mack, M., Müller, M., & Kuchler, K. (2012). Type I interferons promote fatal immunopathology by regulating inflammatory monocytes and neutrophils during Candida infections. PLoS pathogens, 8(7), e1002811. https://doi.org/10.1371/journal.ppat.1002811
46. Martíez-Force, E., & Benítez, T. (1992). Changes in yeast amino acid pool with respiratory versus fermentative metabolism. Biotechnology and bioengineering, 40(6), 643–649. https://doi.org/10.1002/bit.260400602
47. Martin, R., Albrecht-Eckardt, D., Brunke, S., Hube, B., Hünniger, K., & Kurzai, O. (2013). A core filamentation response network in Candida albicans is restricted to eight genes. PloS one, 8(3), e58613. https://doi.org/10.1371/journal.pone.0058613
48. May, R. C., & Casadevall, A. (2018). In Fungal Intracellular Pathogenesis, Form Determines Fate. mBio, 9(5), e02092-18. https://doi.org/10.1128/mBio.02092-18
49. Min, K., Neiman, A. M., & Konopka, J. B. (2020). Fungal Pathogens: Shape-Shifting Invaders. Trends in microbiology, 28(11), 922–933. https://doi.org/10.1016/j.tim.2020.05.001
50. Monniot, C., Boisramé, A., Da Costa, G., Chauvel, M., Sautour, M., Bougnoux, M. E., Bellon-Fontaine, M. N., Dalle, F., d'Enfert, C., & Richard, M. L. (2013). Rbt1 protein domains analysis in Candida albicans brings insights into hyphal surface modifications and Rbt1 potential role during adhesion and biofilm formation. PloS one, 8(12), e82395. https://doi.org/10.1371/journal.pone.0082395
51. Moyes, D. L., Wilson, D., Richardson, J. P., Mogavero, S., Tang, S. X., Wernecke, J., Höfs, S., Gratacap, R. L., Robbins, J., Runglall, M., Murciano, C., Blagojevic, M., Thavaraj, S., Förster, T. M., Hebecker, B., Kasper, L., Vizcay, G., Iancu, S. I., Kichik, N., Häder, A., … Naglik, J. R. (2016). Candidalysin is a fungal peptide toxin critical for mucosal infection. Nature, 532(7597), 64–68. https://doi.org/10.1038/nature17625
52. Nantel, A., Dignard, D., Bachewich, C., Harcus, D., Marcil, A., Bouin, A. P., Sensen, C. W., Hogues, H., van het Hoog, M., Gordon, P., Rigby, T., Benoit, F., Tessier, D. C., Thomas, D. Y., & Whiteway, M. (2002). Transcription profiling of Candida albicans cells undergoing the yeast-to-hyphal transition. Molecular biology of the cell, 13(10), 3452–3465. https://doi.org/10.1091/mbc.e02-05-0272
53. Naranjo-Ortiz, M. A., & Gabaldón, T. (2019). Fungal evolution: major ecological adaptations and evolutionary transitions. Biological reviews of the Cambridge Philosophical Society, 94(4), 1443–1476. https://doi.org/10.1111/brv.12510
54. Netea, M. G., Van Der Graaf, C. A., Vonk, A. G., Verschueren, I., Van Der Meer, J. W., & Kullberg, B. J. (2002). The role of toll-like receptor (TLR) 2 and TLR4 in the host defense

against disseminated candidiasis. The Journal of infectious diseases, 185(10), 1483–1489. https://doi.org/10.1086/340511

55. Newcomb, L. L., Diderich, J. A., Slattery, M. G., & Heideman, W. (2003). Glucose regulation of Saccharomyces cerevisiae cell cycle genes. Eukaryotic cell, 2(1), 143–149. https://doi.org/10.1128/EC.2.1.143-149.2003
56. Palková, Z., & Váchová, L. (2006). Life within a community: benefit to yeast long-term survival. FEMS microbiology reviews, 30(5), 806–824. https://doi.org/10.1111/j.1574-6976.2006.00034.x
57. Pan, X., Harashima, T., & Heitman, J. (2000). Signal transduction cascades regulating pseudohyphal differentiation of Saccharomyces cerevisiae. Current opinion in microbiology, 3(6), 567–572. https://doi.org/10.1016/s1369-5274(00)00142-9
58. Pappas, P. G., Lionakis, M. S., Arendrup, M. C., Ostrosky-Zeichner, L., & Kullberg, B. J. (2018). Invasive candidiasis. Nature reviews. Disease primers, 4, 18026. https://doi.org/10.1038/nrdp.2018.26
59. Peeters, K., Van Leemputte, F., Fischer, B., Bonini, B. M., Quezada, H., Tsytlonok, M., Haesen, D., Vanthienen, W., Bernardes, N., Gonzalez-Blas, C. B., Janssens, V., Tompa, P., Versées, W., & Thevelein, J. M. (2017). Fructose-1,6-bisphosphate couples glycolytic flux to activation of Ras. Nature communications, 8(1), 922. https://doi.org/10.1038/s41467-017-01019-z
60. Pradhan, B., Guha, D., Ray, P., Das, D., & Aich, P. (2016). Comparative Analysis of the Effects of Two Probiotic Bacterial Strains on Metabolism and Innate Immunity in the RAW 264.7 Murine Macrophage Cell Line. Probiotics and antimicrobial proteins, 8(2), 73–84. https://doi.org/10.1007/s12602-016-9211-4
61. Puumala, E., Fallah, S., Robbins, N., & Cowen, L. E. (2024). Advancements and challenges in antifungal therapeutic development. Clinical microbiology reviews, 37(1), e0014223. https://doi.org/10.1128/cmr.00142-23
62. Reuss, O., Vik, A., Kolter, R., & Morschhäuser, J. (2004). The SAT1 flipper, an optimized tool for gene disruption in Candida albicans. Gene, 341, 119–127. https://doi.org/10.1016/j.gene.2004.06.021
63. Richardson, J. P., Mogavero, S., Moyes, D. L., Blagojevic, M., Krüger, T., Verma, A. H., Coleman, B. M., De La Cruz Diaz, J., Schulz, D., Ponde, N. O., Carrano, G., Kniemeyer, O., Wilson, D., Bader, O., Enoiu, S. I., Ho, J., Kichik, N., Gaffen, S. L., Hube, B., & Naglik, J. R. (2018). Processing of Candida albicans Ece1p Is Critical for Candidalysin Maturation and Fungal Virulence. mBio, 9(1), e02178-17. https://doi.org/10.1128/mBio.02178-17
64. Riquelme, M., Aguirre, J., Bartnicki-García, S., Braus, G. H., Feldbrügge, M., Fleig, U., Hansberg, W., Herrera-Estrella, A., Kämper, J., Kück, U., Mouriño-Pérez, R. R., Takeshita, N., & Fischer, R. (2018). Fungal Morphogenesis, from the Polarized Growth of Hyphae to Complex Reproduction and Infection Structures. Microbiology and molecular biology reviews : MMBR, 82(2), e00068-17. https://doi.org/10.1128/MMBR.00068-17
65. Rolland, F., De Winde, J. H., Lemaire, K., Boles, E., Thevelein, J. M., & Winderickx, J. (2000). Glucose-induced cAMP signalling in yeast requires both a G-protein coupled receptor system for extracellular glucose detection and a separable hexose kinase-dependent sensing process. Molecular microbiology, 38(2), 348–358. https://doi.org/10.1046/j.1365-2958.2000.02125.x
66. Rouillon, A., Barbey, R., Patton, E. E., Tyers, M., & Thomas, D. (2000). Feedback-regulated degradation of the transcriptional activator Met4 is triggered by the SCF(Met30)complex. The EMBO journal, 19(2), 282–294. https://doi.org/10.1093/emboj/19.2.282
67. Ryan, O., Shapiro, R. S., Kurat, C. F., Mayhew, D., Baryshnikova, A., Chin, B., Lin, Z. Y., Cox, M. J., Vizeacoumar, F., Cheung, D., Bahr, S., Tsui, K., Tebbji, F., Sellam, A., Istel, F., Schwarzmüller, T., Reynolds, T. B., Kuchler, K., Gifford, D. K., Whiteway, M., … Boone, C. (2012). Global gene deletion analysis exploring yeast filamentous growth. Science (New York, N.Y.), 337(6100), 1353–1356. https://doi.org/10.1126/science.1224339
68. Sánchez-Martínez, C., & Pérez-Martín, J. (2002). Gpa2, a G-protein alpha subunit required for hyphal development in Candida albicans. Eukaryotic cell, 1(6), 865–874. https://doi.org/10.1128/EC.1.6.865-874.2002
69. Schiestl, R. H., & Gietz, R. D. (1989). High efficiency transformation of intact yeast cells using single stranded nucleic acids as a carrier. Current genetics, 16(5-6), 339–346. https://doi.org/10.1007/BF00340712

70. Schröder, M., Chang, J. S., & Kaufman, R. J. (2000). The unfolded protein response represses nitrogen-starvation induced developmental differentiation in yeast. Genes & development, 14(23), 2962–2975. https://doi.org/10.1101/gad.852300
71. Segal, E., & Frenkel, M. (2018). Experimental in Vivo Models of Candidiasis. Journal of fungi (Basel, Switzerland), 4(1), 21. https://doi.org/10.3390/jof4010021
72. Sexton, A. C., & Howlett, B. J. (2006). Parallels in fungal pathogenesis on plant and animal hosts. Eukaryotic cell, 5(12), 1941–1949. https://doi.org/10.1128/EC.00277-06
73. Sharkey, L. L., McNemar, M. D., Saporito-Irwin, S. M., Sypherd, P. S., & Fonzi, W. A. (1999). HWP1 functions in the morphological development of Candida albicans downstream of EFG1, TUP1, and RBF1. Journal of bacteriology, 181(17), 5273–5279. https://doi.org/10.1128/JB.181.17.5273-5279.1999
74. Shee, S., Singh, S., Tripathi, A., Thakur, C., Kumar T, A., Das, M., Yadav, V., Kohli, S., Rajmani, R. S., Chandra, N., Chakrapani, H., Drlica, K., & Singh, A. (2022). Moxifloxacin-Mediated Killing of Mycobacterium tuberculosis Involves Respiratory Downshift, Reductive Stress, and Accumulation of Reactive Oxygen Species. Antimicrobial agents and chemotherapy, 66(9), e0059222. https://doi.org/10.1128/aac.00592-22
75. Shrivastava, M., Feng, J., Coles, M., Clark, B., Islam, A., Dumeaux, V., & Whiteway, M. (2021). Modulation of the complex regulatory network for methionine biosynthesis in fungi. Genetics, 217(2), iyaa049. https://doi.org/10.1093/genetics/iyaa049
76. Smith, M. G., Des Etages, S. G., & Snyder, M. (2004). Microbial synergy via an ethanol-triggered pathway. Molecular and cellular biology, 24(9), 3874–3884. https://doi.org/10.1128/MCB.24.9.3874-3884.2004
77. Smothers, D. B., Kozubowski, L., Dixon, C., Goebl, M. G., & Mathias, N. (2000). The abundance of Met30p limits SCF(Met30p) complex activity and is regulated by methionine availability. Molecular and cellular biology, 20(21), 7845–7852. https://doi.org/10.1128/MCB.20.21.7845-7852.2000
78. Song, Y., Li, S., Zhao, Y., Zhang, Y., Lv, Y., Jiang, Y., Wang, Y., Li, D., & Zhang, H. (2019). ADH1 promotes Candida albicans pathogenicity by stimulating oxidative phosphorylation. International journal of medical microbiology : IJMM, 309(6), 151330. https://doi.org/10.1016/j.ijmm.2019.151330
79. Strudwick, N., Brown, M., Parmar, V. M., & Schröder, M. (2010). Ime1 and Ime2 are required for pseudohyphal growth of Saccharomyces cerevisiae on nonfermentable carbon sources. Molecular and cellular biology, 30(23), 5514–5530. https://doi.org/10.1128/MCB.00390-10
80. Su, C., Yu, J., Sun, Q., Liu, Q., & Lu, Y. (2018). Hyphal induction under the condition without inoculation in Candida albicans is triggered by Brg1-mediated removal of NRG1 inhibition. Molecular microbiology, 108(4), 410–423. https://doi.org/10.1111/mmi.13944
81. Su, N. Y., Ouni, I., Papagiannis, C. V., & Kaiser, P. (2008). A dominant suppressor mutation of the met30 cell cycle defect suggests regulation of the Saccharomyces cerevisiae Met4-Cbf1 transcription complex by Met32. The Journal of biological chemistry, 283(17), 11615–11624. https://doi.org/10.1074/jbc.M708230200
82. Thomas, D., & Surdin-Kerjan, Y. (1997). Metabolism of sulfur amino acids in Saccharomyces cerevisiae. Microbiology and molecular biology reviews : MMBR, 61(4), 503–532. https://doi.org/10.1128/mmbr.61.4.503-532.1997
83. Thompson, D. S., Carlisle, P. L., & Kadosh, D. (2011). Coevolution of morphology and virulence in Candida species. Eukaryotic cell, 10(9), 1173–1182. https://doi.org/10.1128/EC.05085-11
84. Uwamahoro, N., Verma-Gaur, J., Shen, H. H., Qu, Y., Lewis, R., Lu, J., Bambery, K., Masters, S. L., Vince, J. E., Naderer, T., & Traven, A. (2014). The pathogen Candida albicans hijacks pyroptosis for escape from macrophages. mBio, 5(2), e00003–e14. https://doi.org/10.1128/mBio.00003-14
85. Van de Velde, S., & Thevelein, J. M. (2008). Cyclic AMP-protein kinase A and Snf1 signaling mechanisms underlie the superior potency of sucrose for induction of filamentation in Saccharomyces cerevisiae. Eukaryotic cell, 7(2), 286–293. https://doi.org/10.1128/EC.00276-07
86. Wang, L., & Lin, X. (2012). Morphogenesis in fungal pathogenicity: shape, size, and surface. PLoS pathogens, 8(12), e1003027. https://doi.org/10.1371/journal.ppat.1003027
87. Wilson, D., Naglik, J. R., & Hube, B. (2016). The Missing Link between Candida albicans Hyphal Morphogenesis and Host Cell Damage. PLoS pathogens, 12(10), e1005867. https://doi.org/10.1371/journal.ppat.1005867

88. Winer, J., Jung, C. K., Shackel, I., & Williams, P. M. (1999). Development and validation of real-time quantitative reverse transcriptase-polymerase chain reaction for monitoring gene expression in cardiac myocytes in vitro. Analytical biochemistry, 270(1), 41–49. https://doi.org/10.1006/abio.1999.4085
89. Wu, J., Zhang, N., Hayes, A., Panoutsopoulou, K., & Oliver, S. G. (2004). Global analysis of nutrient control of gene expression in Saccharomyces cerevisiae during growth and starvation. Proceedings of the National Academy of Sciences of the United States of America, 101(9), 3148–3153. https://doi.org/10.1073/pnas.0308321100
90. Wu, Y., Zhang, S., Gong, X., Yu, Q., Zhang, Y., Luo, M., Zhang, X., Workman, J. L., Yu, X., & Li, S. (2019). Glycolysis regulates gene expression by promoting the crosstalk between H3K4 trimethylation and H3K14 acetylation in Saccharomyces cerevisiae. Journal of genetics and genomics = Yi chuan xue bao, 46(12), 561–574. https://doi.org/10.1016/j.jgg.2019.11.007
91. Xue, Y., Batlle, M., & Hirsch, J. P. (1998). GPR1 encodes a putative G protein-coupled receptor that associates with the Gpa2p Galpha subunit and functions in a Ras-independent pathway. The EMBO journal, 17(7), 1996–2007. https://doi.org/10.1093/emboj/17.7.1996
92. Yen, J. L., Su, N. Y., & Kaiser, P. (2005). The yeast ubiquitin ligase SCFMet30 regulates heavy metal response. Molecular biology of the cell, 16(4), 1872–1882. https://doi.org/10.1091/mbc.e04-12-1130
93. Yoshino, M., & Murakami, K. (1982). AMP deaminase as a control system of glycolysis in yeast. Mechanism of the inhibition of glycolysis by fatty acid and citrate. The Journal of biological chemistry, 257(18), 10644–10649.
94. Yun, C. W., Tamaki, H., Nakayama, R., Yamamoto, K., & Kumagai, H. (1997). G-protein coupled receptor from yeast Saccharomyces cerevisiae. Biochemical and biophysical research communications, 240(2), 287–292. https://doi.org/10.1006/bbrc.1997.7649

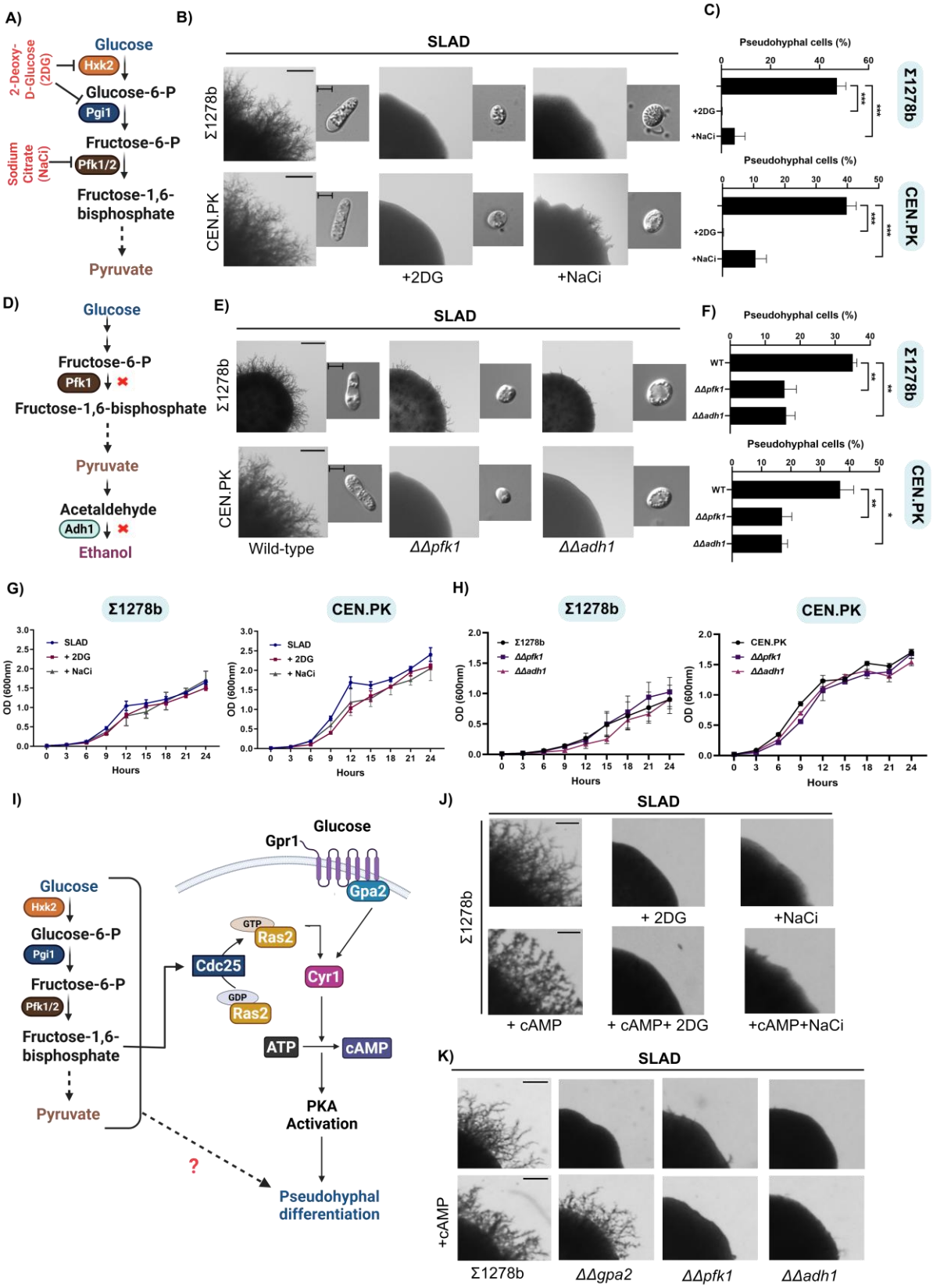

Figure 1. Glycolysis is Critical for Pseudohyphal Differentiation in a cAMP-PKA Independent Manner in *S. cerevisiae*.

(A) Schematic overview of glycolysis and its inhibition by glycolysis inhibitors (2-Deoxy-D-Glucose (2DG) and sodium citrate (NaCi)). **(B)** Wild-type Σ1278b or CEN.PK were spotted on nitrogen-

limiting medium containing 2% glucose (SLAD) with and without sub-inhibitory concentrations of glycolysis inhibitors (2-Deoxy-D-Glucose (2DG) and sodium citrate (NaCi)), incubated for 10 days at 30 °C. Whole colony imaging was done using Olympus MVX10 stereo microscope and single cell imaging was done using Zeiss Apotome microscope. Scale bar represents 1mm for whole colony images and 5µm for single cell images. **(C)** Cells from colonies were isolated and single cells were imaged using Zeiss Apotome microscope and percentage of pseudohyphal cells were calculated using ImageJ. More than 500 cells were counted for each condition. Statistical analysis was done using one-way ANOVA test, ***($P<0.001$). Error bars represent SEM. **(D)** Schematic overview of glycolysis showing targeted gene deletions. **(E)** Pertinent knockout strains which lack genes encoding for enzymes involved in glycolysis such as *pfk1* and *adh1* were spotted on SLAD along with wild-type ∑1278b or CEN.PK. Whole colony imaging was done using Olympus MVX10 stereo microscope and single cell imaging was done using Zeiss Apotome microscope. Scale bar represents 1mm for whole colony images and 5µm for single cell images. **(F)** Cells from colonies were isolated and single cells were imaged using Zeiss Apotome microscope and percentage of pseudohyphal cells were calculated using ImageJ. More than 500 cells were counted for each strains. Statistical analysis was done using one-way ANOVA test, **($P<0.01$) and *($P<0.05$). Error bars represent SEM. **(G)** Growth curve was performed to monitor overall growth of wild-type strains on SLAD, SLAD+2DG and SLAD+NaCi. Overnight grown culture of wild-type strains (∑1278b or CEN.PK) were diluted to OD_{600}=0.01 in fresh SLAD medium with and without 2DG (0.05%) or NaCi (0.5%) and allowed to grow at 30 °C for 24 hours. OD_{600} was recorded at 3-h intervals **(H)** Growth curve was performed to monitor overall growth of wild-type and knockout strains on SLAD. Overnight grown culture of deletion strains (*ΔΔpfk1* or *ΔΔadh1*) along with wild-type strains (∑1278b or CEN.PK) were diluted to OD_{600}=0.01 in fresh SLAD and allowed to grow at 30 °C for 24 hours. OD_{600} was recorded at 3-h intervals. **(I)** Schematic overview of the role of glucose and glycolytic intermediates in the activation of cAMP-PKA pathway during pseudohyphal differentiation. **(J)** Wild-type ∑1278b was spotted on SLAD containing sub-inhibitory concentration of 2DG or NaCi with and without cAMP (1mM), incubated for 10 days at 30 °C. After 10 days, whole colony imaging was done using Olympus MVX10 stereo microscope. Scale bar represents 1mm for whole colony images. **(K)** Pertinent knockout strains which lack genes that encode for enzymes involved in glycolysis such as *pfk1* and *adh1* were spotted on SLAD with and without cAMP (1mM), incubated for 10 days at 30 °C. *ΔΔgpa2* strain was used as a control. After 10 days, whole colony imaging was done using Olympus MVX10 stereo microscope. Scale bar represents 1mm for whole colony images.

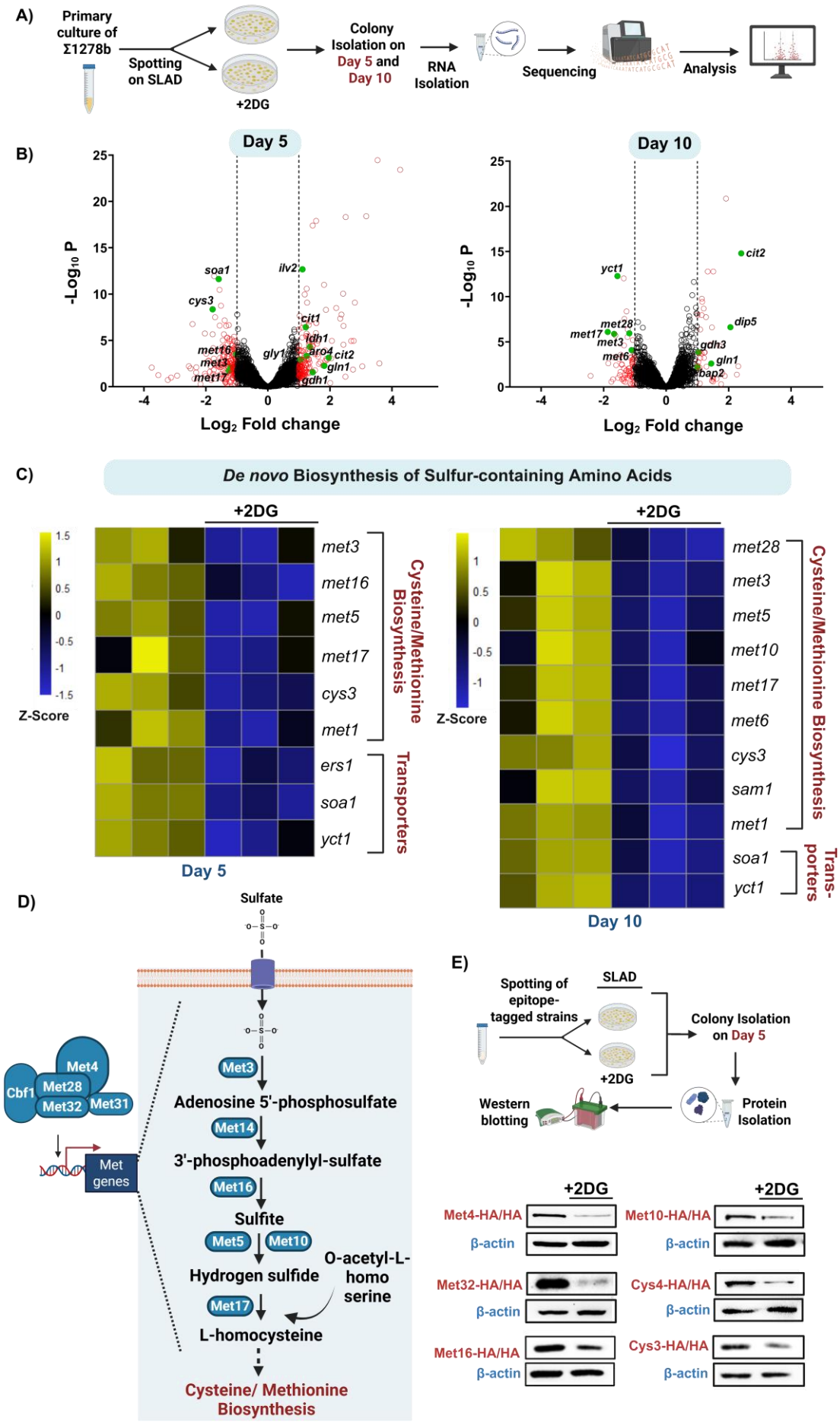
A)
Primary culture of Σ1278b
Spotting on SLAD
+2DG
Colony Isolation on Day 5 and Day 10
RNA Isolation
Sequencing
Analysis
B)
Day 5
Day 10
-Log10 P
Log2 Fold change
soa1
cys3
ilv2
cit1
idh1
aro4
cit2
gln1
gdh1
met16
met3
met17
gly1
yct1
met28
met6
dip5
gdh3
bap2
C)
De novo Biosynthesis of Sulfur-containing Amino Acids
+2DG
Z-Score
met3
met16
met5
met17
cys3
met1
ers1
soa1
yct1
Cysteine/Methionine Biosynthesis
Transporters
Day 5
met28
met3
met5
met10
met17
met6
cys3
sam1
met1
soa1
yct1
Trans-porters
Day 10
D)
Sulfate
Cbf1
Met4
Met28
Met32
Met31
Met genes
Met3
Adenosine 5'-phosphosulfate
Met14
3'-phosphoadenylyl-sulfate
Met16
Sulfite
Met5
Met10
Hydrogen sulfide
O-acetyl-L-homo serine
Met17
L-homocysteine
Cysteine/ Methionine Biosynthesis
E)
Spotting of epitope-tagged strains
SLAD
+2DG
Colony Isolation on Day 5
Protein Isolation
Western blotting
Met4-HA/HA
Met10-HA/HA
Met32-HA/HA
Cys4-HA/HA
Met16-HA/HA
Cys3-HA/HA
β-actin

1652

Figure 2. Comparative Transcriptomics Identifies the Role of Glycolysis in Regulating Sulfur Metabolism During Pseudohyphal Differentiation in *S. cerevisiae*.

(A) Schematic overview of steps involved in RNA isolation and RNA-sequencing. **(B)** Volcano plots represent differentially expressed genes in 2DG treated cells compared to untreated cells isolated from D-5 and D-10 colonies, respectively. Genes which are upregulated (Log_2 fold change ≥ 1) and downregulated (Log_2 fold change ≤ -1) are highlighted in red. Some of the significantly upregulated and downregulated genes involved in the biosynthesis of various amino acids are highlighted in green. **(C)** Heatmaps represent the differentially expressed genes involved in *de novo* biosynthesis and transport of sulfur-containing amino acids, in 2DG treated cells compared to untreated cells isolated from D-5 and D-10 colonies, respectively (n=3). Scale bar represents Z-Score. **(D)** Schematic overview of *de novo* biosynthesis of sulfur-containing amino acids. **(E)** Schematic overview of steps involved in the Western blotting experiments. Epitope-tagged strains of various proteins involved in the *de novo* biosynthesis of sulfur-containing amino acids including Met4, Met32, Met16, Met10, Cys4 and Cys3 were spotted on SLAD in the presence and absence of sub-inhibitory concentration of 2DG following which, cells from colonies were isolated on D-5 and levels of these proteins were assessed using Western blotting (n=3). β-actin was used as loading control.

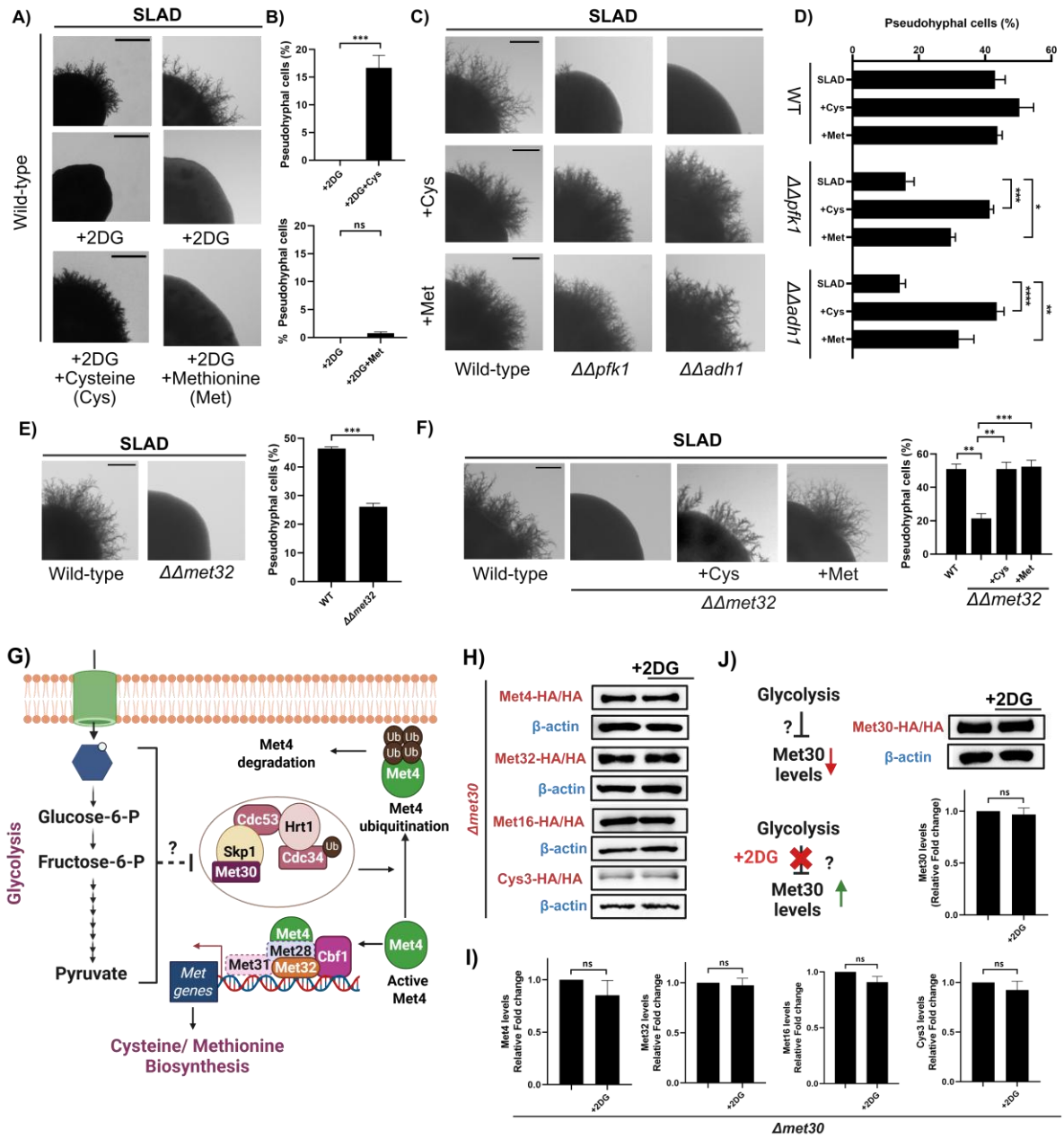

Figure 3. Glycolysis-mediated Regulation of Sulfur Metabolism is Critical for Pseudohyphal Differentiation in *S. cerevisiae*.

(A) Wild-type ∑1278b was spotted on SLAD containing sub-inhibitory concentration of 2DG with and without sulfur-containing compounds including cysteine (500μM) or methionine (20μM), incubated for 10 days at 30 °C. After 10 days, whole colony imaging was done using Olympus MVX10 stereo microscope. Scale bar represents 1mm for whole colony images. **(B)** Cells from colonies were isolated and single cells were imaged using Zeiss Apotome microscope and percentage of pseudohyphal cells were calculated using ImageJ. More than 500 cells were counted for each condition. Statistical analysis was done using unpaired t-test, ***(P<0.001) and ns (non-significant). Error bars represent SEM. **(C)** Pertinent knockout strains which lack genes encoding for enzymes involved in glycolysis such as *pfk1* and *adh1* along with wild-type were spotted on SLAD with and without sulfur-containing compounds including cysteine (200μM) or methionine (20μM), incubated for 10 days at 30 °C. After 10 days, whole colony imaging was done using Olympus MVX10 stereo microscope. Scale bar represents 1mm for whole colony images. **(D)** Cells from colonies were isolated and single cells were imaged using Zeiss Apotome microscope and percentage of

pseudohyphal cells were calculated using ImageJ. More than 500 cells were counted for each condition. Statistical analysis was done using one-way ANOVA test, ****(P<0.0001), ***(P<0.001), **(P<0.01) and *(P<0.05). Error bars represent SEM. **(E)** Pertinent knockout strains which lack genes encoding for transcription factor involved in *de novo* biosynthesis of sulfur-containing amino acids including *met32* along with wild-type ∑1278b were spotted on SLAD and imaged after 10 days using Olympus MVX10 stereo microscope. Scale bar represents 1mm for whole colony images. Cells from colonies were isolated and single cells were imaged using Zeiss Apotome microscope and percentage of pseudohyphal cells were calculated using ImageJ. More than 500 cells were counted for each condition. Statistical analysis was done using unpaired t-test, ***(P<0.001). Error bars represent SEM. **(F)** Pertinent knockout strain *ΔΔmet32* was spotted on SLAD with and without sulfur-containing compounds including cysteine (200μM) or methionine (20μM), incubated for 10 days at 30 °C. Wild-type spotted on SLAD was used as control. After 10 days, imaging was done using Olympus MVX10 stereo microscope. Scale bar represents 1mm for whole colony images. Cells from colonies were isolated and single cells were imaged using Zeiss Apotome microscope and percentage of pseudohyphal cells were calculated using ImageJ. More than 500 cells were counted for each condition. Statistical analysis was done using one-way ANOVA test, ***(P<0.001) and **(P<0.01). Error bars represent SEM. **(G)** Schematic overview of the proposed role of SCF^{Met30} in glycolysis-dependent regulation of sulfur metabolism during pseudohyphal differentiation under nitrogen-limiting conditions in *S. cerevisiae.* **(H)** Epitope-tagged strains of various proteins involved in the *de novo* biosynthesis of sulfur-containing amino acids including Met4, Met32, Met16 and Cys3 in *Δmet30* background were spotted on SLAD in the presence and absence of sub-inhibitory concentration of 2DG following which, cells from colonies were isolated on D-5 and levels of these proteins were assessed using Western blotting (n=3). β-actin was used as loading control. **(I)** Raw images of Western blots were analysed using ImageJ to normalize targeted protein expression with the expression of housekeeping protein- β-actin, in order to generate densitometric graphs. Statistical analysis was done using unpaired t-test, ns (non-significant). Error bars represent SEM. **(J)** Epitope-tagged strain of Met30 was spotted on SLAD in the presence and absence of sub-inhibitory concentration of 2DG following which, cells from colonies were isolated on D-5 and levels of these proteins were assessed using Western blotting (n=3). β-actin was used as loading control. Raw images of Western blots were analysed using ImageJ to normalize targeted protein expression with the expression of housekeeping protein- β-actin, in order to generate densitometric graphs. Statistical analysis was done using unpaired t-test, ns (non-significant). Error bars represent SEM.

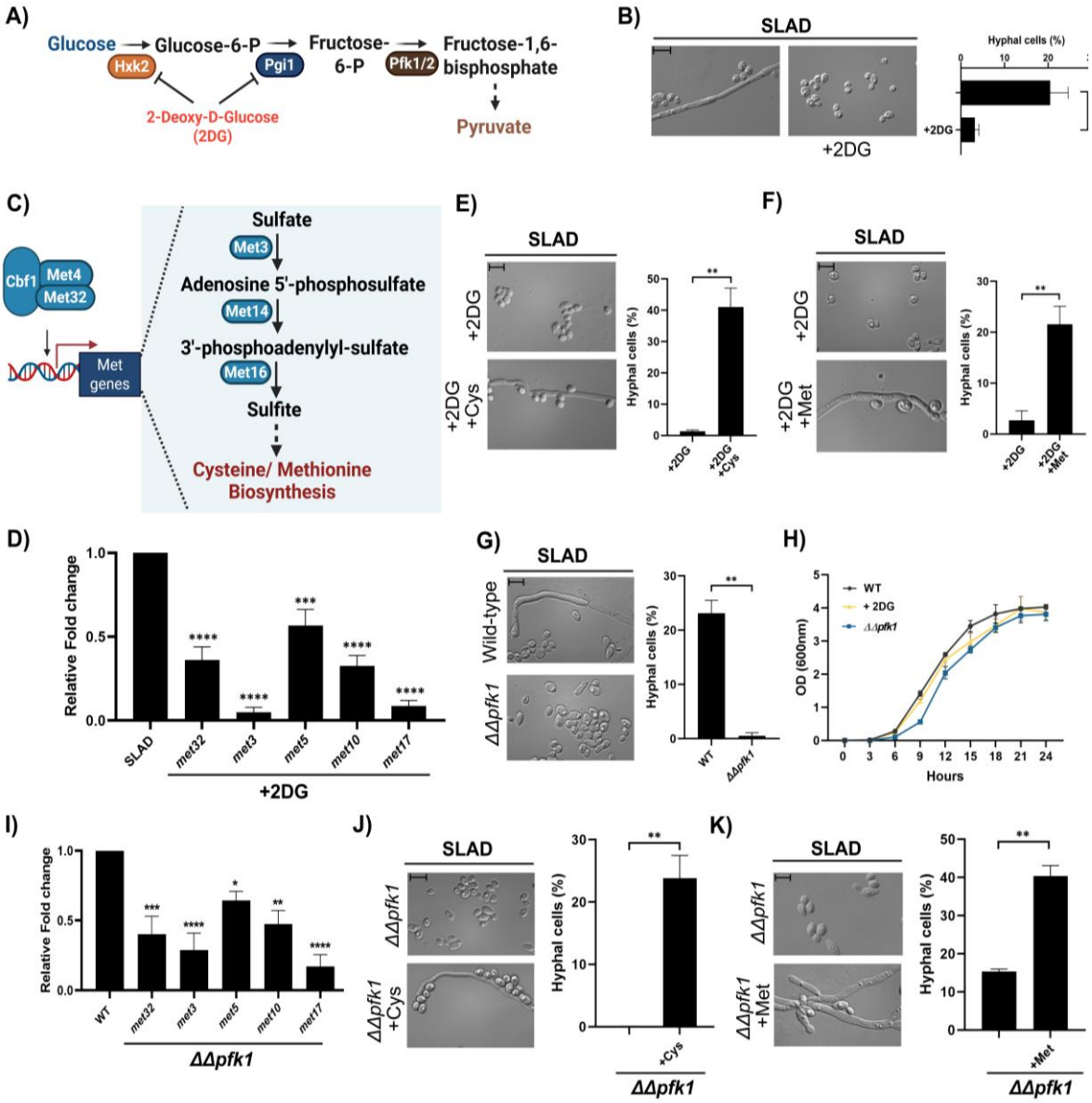

Figure 4. Glycolysis-dependent Sulfur Metabolism is Critical for Hyphal Differentiation in *C. albicans*.

(A) Schematic overview of glycolysis and its inhibition by glycolysis inhibitor (2-Deoxy-D-Glucose (2DG) **(B)** Wild-type SC5314 was spotted on SLAD with and without sub-inhibitory concentration of glycolysis inhibitor 2DG, incubated for 7 days at 37 °C. Cells from colonies were isolated and single cells were imaged using Zeiss Apotome microscope and percentage of hyphal cells were calculated using ImageJ. More than 500 cells were counted for each condition. Scale bar represents 10μm for single cell images. Statistical analysis was done using unpaired t-test, **(P<0.01). Error bars represent SEM. **(C)** Schematic overview of *de novo* biosynthesis of sulfur-containing amino acids. **(D)** Wild-type SC5314 was spotted on SLAD, in the presence and absence of sub-inhibitory concentration of 2DG and cells from colonies were isolated after ~4 days, for RNA isolation. We then performed comparative RT-qPCR to check for the relative expression of genes involved in the *de novo* biosynthesis of sulfur-containing amino acids pathway including *met32*, *met3*, *met5* (*ecm17*), *met10* and *met17* (*met15*). Statistical analysis was done using one-way ANOVA test, ****(P<0.0001) and ***(P<0.001). Error bars represent SEM. **(E)** Wild-type SC5314 was spotted on SLAD containing sub-inhibitory concentration of 2DG with and without cysteine (100μM) and, incubated for 7 days at 37 °C. Cells from colonies were isolated and single cells were imaged using Zeiss Apotome microscope and percentage of hyphal cells were calculated using ImageJ. Scale bar

represents 10μm for single cell images. More than 500 cells were counted for each condition. Statistical analysis was done using unpaired t-test, **(P<0.01). Error bars represent SEM. **(F)** Wild-type SC5314 was spotted on SLAD containing sub-inhibitory concentration of 2DG with and without methionine (20μM) and, incubated for 7 days at 37 °C. Cells from colonies were isolated and single cells were imaged using Zeiss Apotome microscope and percentage of hyphal cells were calculated using ImageJ. More than 500 cells were counted for each condition. Scale bar represents 10μm for single cell images. Statistical analysis was done using unpaired t-test, **(P<0.01). Error bars represent SEM. **(G)** Wild-type SC5314 and pertinent knockout strain which lacks the genes encoding for a glycolytic enzyme, *pfk1* (*ΔΔpfk1*) were spotted on SLAD, incubated for 7 days at 37 °C. Cells from colonies were isolated and single cells were imaged using Zeiss Apotome microscope and percentage of hyphal cells were calculated using ImageJ. Scale bar represents 10μm for single cell images. More than 500 cells were counted for each strain. Statistical analysis was done using unpaired t-test, **(P<0.01). Error bars represent SEM. **(H)** Growth curve was performed to monitor overall growth of wild-type strain on SLAD and SLAD+2DG and *ΔΔpfk1* on SLAD. Overnight grown culture of wild-type strain (SC5314) were diluted to OD_{600}=0.01 in fresh SLAD medium with and without 2DG (0.2%) and allowed to grow at 30 °C for 24 hours. OD_{600} was recorded at 3-h intervals. For *ΔΔpfk1*, overnight grown culture of *ΔΔpfk1* strains along with wild-type strain (SC5314) were diluted to OD_{600}=0.01 in fresh SLAD and allowed to grow at 30 °C for 24 hours. OD_{600} was recorded at 3-h intervals. **(I)** *ΔΔpfk1* along with Wild-type SC5314 was spotted on SLAD and cells from colonies were isolated after ~4 days, for RNA isolation. We then performed comparative RT-qPCR to check for the relative expression of genes involved in the *de novo* biosynthesis of sulfur-containing amino acids pathway including *met32*, *met3*, *met5* (*ecm17*), *met10* and *met17* (*met15*). Statistical analysis was done using one-way ANOVA test, ****(P<0.0001), ***(P<0.001), **(P<0.01) and *(P<0.05). Error bars represent SEM. **(J)** *ΔΔpfk1* was spotted on SLAD in the presence and absence of cysteine (100μM), incubated for 7 days at 37 °C. Cells from colonies were isolated and single cells were imaged using Zeiss Apotome microscope and percentage of hyphal cells were calculated using ImageJ. More than 500 cells were counted for each condition. Statistical analysis was done using unpaired t-test, **(P<0.01). Error bars represent SEM. **(K)** *ΔΔpfk1* was spotted on SLAD in the presence and absence of methionine (10μM), incubated for 7 days at 37 °C. Cells from colonies were isolated and single cells were imaged using Zeiss Apotome microscope and percentage of hyphal cells were calculated using ImageJ. More than 500 cells were counted for each condition. Statistical analysis was done using unpaired t-test, **(P<0.01). Error bars represent SEM.

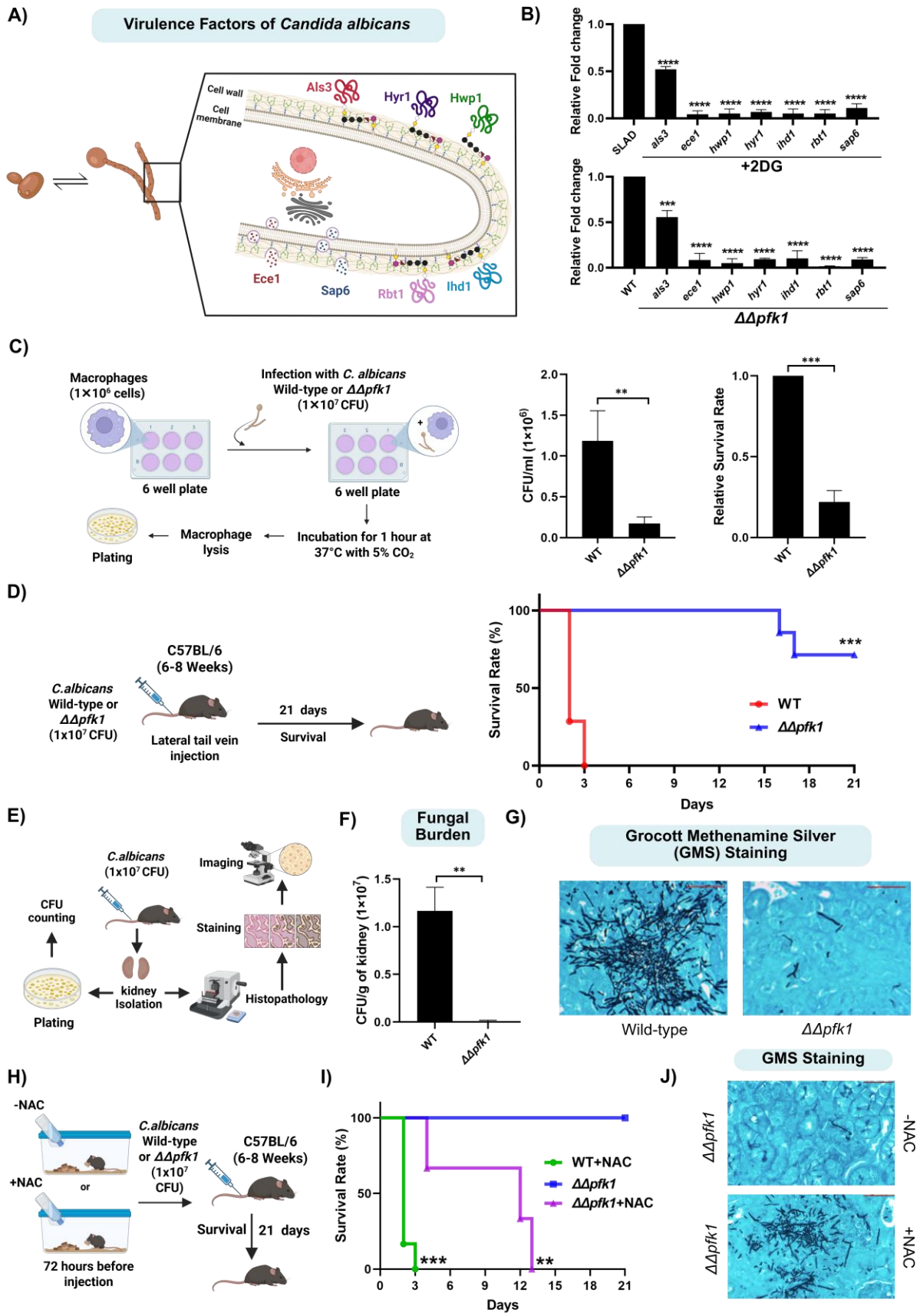
A)
Virulence Factors of Candida albicans
Cell wall
Cell membrane
Als3
Hyr1
Hwp1
Ece1
Sap6
Rbt1
Ihd1
B)
Relative Fold change
SLAD
als3
ece1
hwp1
hyr1
ihd1
rbt1
sap6
+2DG
WT
ΔΔpfk1
C)
Macrophages (1×10⁶ cells)
6 well plate
Infection with C. albicans Wild-type or ΔΔpfk1 (1×10⁷ CFU)
Incubation for 1 hour at 37°C with 5% CO₂
Macrophage lysis
Plating
CFU/ml (1×10⁶)
Relative Survival Rate
D)
C57BL/6 (6-8 Weeks)
C.albicans Wild-type or ΔΔpfk1 (1x10⁷ CFU)
Lateral tail vein injection
21 days
Survival
Survival Rate (%)
Days
WT
ΔΔpfk1
E)
C.albicans (1x10⁷ CFU)
CFU counting
Imaging
Staining
kidney Isolation
Histopathology
Plating
F)
Fungal Burden
CFU/g of kidney (1×10⁷)
G)
Grocott Methenamine Silver (GMS) Staining
Wild-type
ΔΔpfk1
H)
-NAC
+NAC
or
72 hours before injection
C.albicans Wild-type or ΔΔpfk1 (1x10⁷ CFU)
C57BL/6 (6-8 Weeks)
Survival
21 days
I)
Survival Rate (%)
Days
WT+NAC
ΔΔpfk1
ΔΔpfk1+NAC
J)
GMS Staining
ΔΔpfk1
-NAC
+NAC

1847 **Figure 5. Perturbation of Glycolysis Leads to Attenuated Fungal Virulence in *C. albicans*.**
1848
1849 **(A)** Schematic overview of various proteins involved in hyphal differentiation and virulence of
1850 *C. albicans*. **(B)** Wild-type SC5314 was spotted on SLAD, in the presence and absence of sub-
1851 inhibitory concentration of 2DG or wild-type SC5314 and *ΔΔpfk1* were spotted on SLAD and cells
1852 from these colonies were isolated after ~4 days, for RNA isolation. We then performed comparative
1853 RT-qPCR to check for the relative expression of genes involved in hyphal differentiation and virulence
1854 of *C. albicans* including *als3, ece1, hwp1, hyr1, ihd1, rbt1* and *sap6.* Statistical analysis was done
1855 using one-way ANOVA test, ****(P<0.0001) and ***(P<0.001). Error bars represent SEM. **(C)**
1856 Schematic overview of *in vitro* microbial survival assay. *RAW 264.7* macrophages were incubated
1857 with the wild-type and *ΔΔpfk1* strain with MOI=10. After 1 hour of incubation, macrophages were
1858 lysed and plating was done to enumerate CFU. Percentage of survival was expressed as the number
1859 of CFU in the presence of macrophages divided by the number of CFU in the absence of macrophages.
1860 Statistical analysis was done using unpaired t-test, ***(P<0.001) and **(P<0.01). Error bars
1861 represent SEM. **(D)** 6-8-week-old C57BL/6 mice were infected intravenously *via* lateral tail vein
1862 injection with 1×10^7 CFU of wild-type SC5314 or 1×10^7 CFU of *ΔΔpfk1*. To determine survival rate,
1863 mice were monitored for 21 days post-infection for clinical signs of illness or mortality. The results
1864 are representative of seven mice per injected strain. Survival percentage were statistically evaluated
1865 by the Log-rank Mantel-Cox test, ***(P<0.001) (n=7). **(E)** Schematic overview of kidney isolation
1866 to check fungal burden using CFU counting and histology. **(F)** Fungal burden was measured by CFU
1867 counting after kidney isolation from mice injected with either wild-type or *ΔΔpfk1*. Statistical analysis
1868 was done using unpaired t-test, **(P<0.01). Error bars represent SEM. **(G)** Histopathological
1869 analysis of kidney sections using Grocott Methanamine Silver (GMS) staining was done for kidneys
1870 isolated from mice injected with either wild-type SC5314 or *ΔΔpfk1*. Fungal cells appear black in
1871 colour against the colored background of the kidney tissue. Bright field imaging was done using
1872 Axioplan 2 microscope at 40X magnification. Scale bar represents 50 μm. **(H)** Schematic overview
1873 of N-acetyl cysteine (NAC) administration to mice. **(I)** 6mg/ml of NAC was dissolved in distilled
1874 water and administered orally to 6-8-week-old C57BL/6 mice before 72 hours of *C. albicans* infection.
1875 Mice administered with normal distilled water were used as controls. After 72 hours of treatment,
1876 mice were infected intravenously *via* lateral tail vein injection with 1×10^7 CFU of SC5314 or
1877 1×10^7 CFU of *ΔΔpfk1*. To determine survival rate, mice were monitored for 21 days post-infection
1878 for clinical signs of illness or mortality. The results are representative of six mice per condition.
1879 Survival percentage were statistically evaluated by the Log-rank Mantel-Cox test, ***(P<0.001) and
1880 **(P<0.01) (n=6). **(J)** Histopathological analysis of kidney sections using GMS staining was done
1881 for kidneys isolated from mice administrated with normal distilled water or NAC containing distilled
1882 water and injected with *ΔΔpfk1*. Fungal cells appear black in colour against the colored background
1883 of the kidney tissue. Bright field imaging was done using Axioplan 2 microscope at 40X magnification.
1884 Scale bar represents 50 μm.
1885
1886
1887
1888
1889
1890
1891
1892
1893
1894
1895
1896
1897
1898
1899

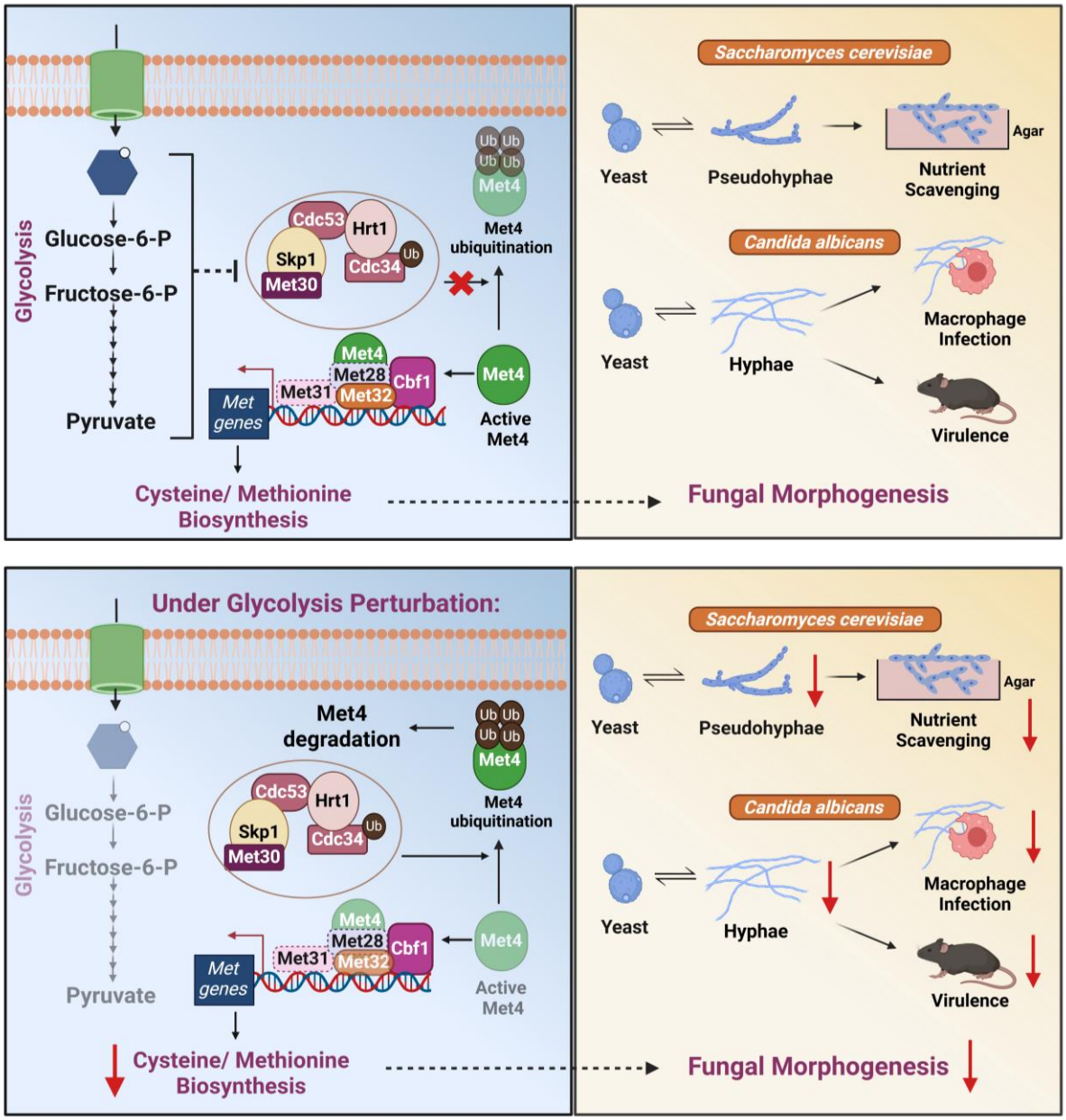

Figure 6. Glycolysis-dependent Sulfur Metabolism Orchestrates Morphological Transitions and Virulence in Fungi.

Active glycolysis plays a key regulatory role in the *de novo* biosynthesis of sulfur-containing amino acids by modulating the activity of SCF^{Met30} complex (SCF^{Met30} complex includes Met30, Skp1, Cdc53, Hrt1 and Cdc34) which in turn affects the expression of genes involved in this process (In *S. cerevisiae*, Met transcription complex includes Met4, Met28, Cbf1, Met31, and Met32, whereas in *C. albicans*, the characterized components of this complex include Met4, Cbf1, and Met32. Hence, Met28 and Met31, unique to the Met transcription complex of *S. cerevisiae* are represented with dotted borders). Glycolysis-dependent sulfur metabolism in turn, is critical for fungal morphogenesis in both species and the ability of *C. albicans* to survive within macrophages and cause systemic infection in a *murine* model of candidiasis. Perturbation of active glycolysis increases Met30 activity, which leads to the increased degradation of Met4, resulting in the reduced expression of genes involved in the *de novo* biosynthesis of sulfur-containing amino acids. This in turn attenuates fungal morphogenesis in both species and the ability of *C. albicans* to survive within macrophages and cause systemic infection in a *murine* model of candidiasis.

Supporting Information

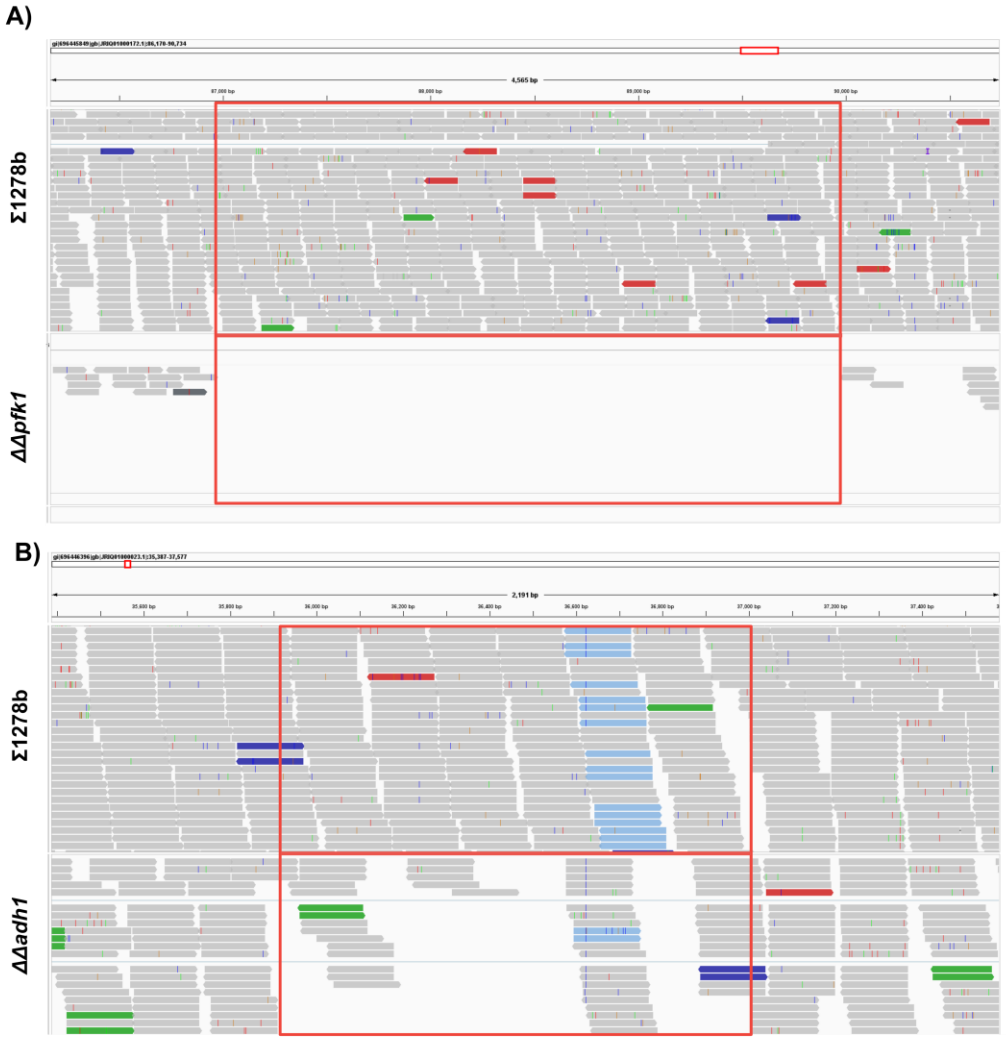

Figure Supplement 1. Confirmation of *pfk1* and *adh1* Deletion in *S. cerevisiae*.

(A) Confirmation of *ΔΔpfk1* strain using whole genome sequencing. IGV software (version 2.16.2) was used for data visualisation. Red box represents gene locus of *pfk1* in wild-type (∑1278b) and *ΔΔpfk1* strains. **(B)** Confirmation of *ΔΔadh1* strain using whole genome sequencing. IGV software (version 2.16.2) was used for data visualisation. Red box represents gene locus of *adh1* in wild-type (∑1278b) and *ΔΔadh1* strains.

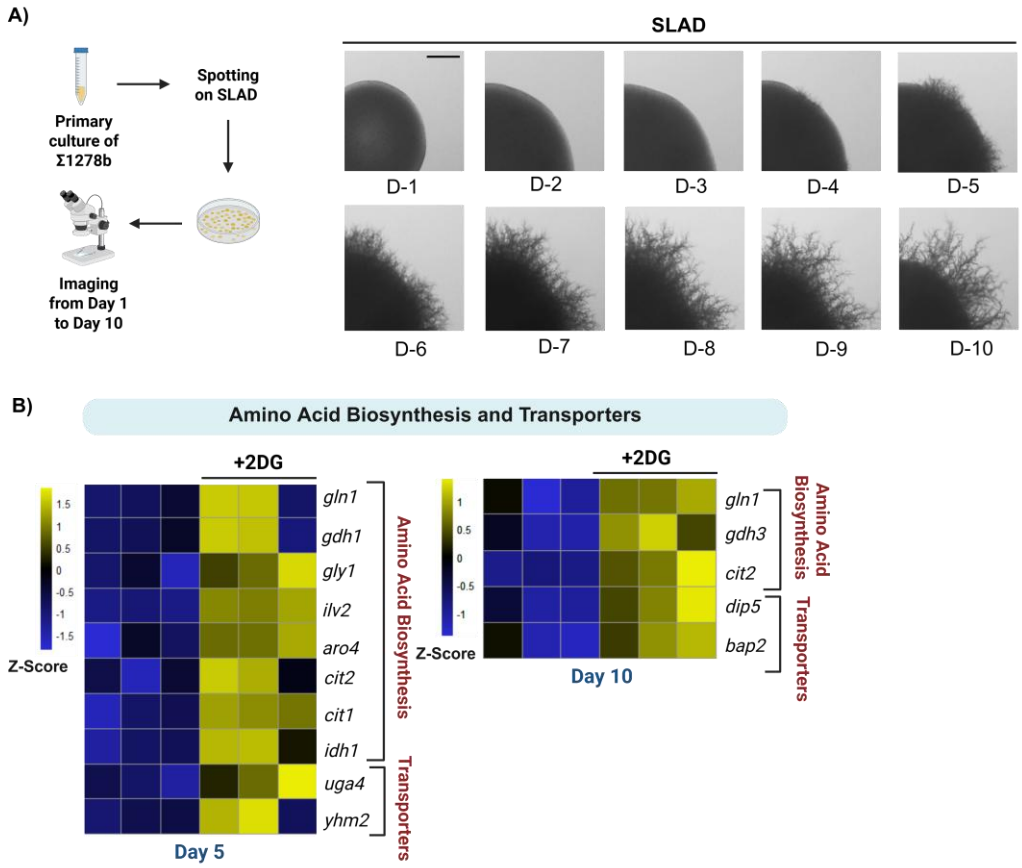

Figure Supplement 2. Comparative Transcriptomics Identifies the Role of Glycolysis During Pseudohypal Differentiation in *S. cerevisiae*.

(A) Wild-type ∑1278b was spotted on SLAD, incubated for 10 days at 30 °C. Colonies were imaged every day, for 10 consecutive days (D-1 to D-10), using Olympus MVX10 stereo microscope. Scale bar represents 1mm for whole colony images. **(B)** Heatmaps represent the differentially expressed genes involved in amino acid biosynthesis and transporters, in 2DG treated cells compared to untreated cells isolated from D-5 and D-10 colonies, respectively (n=3). Scale bar represents Z-Score.

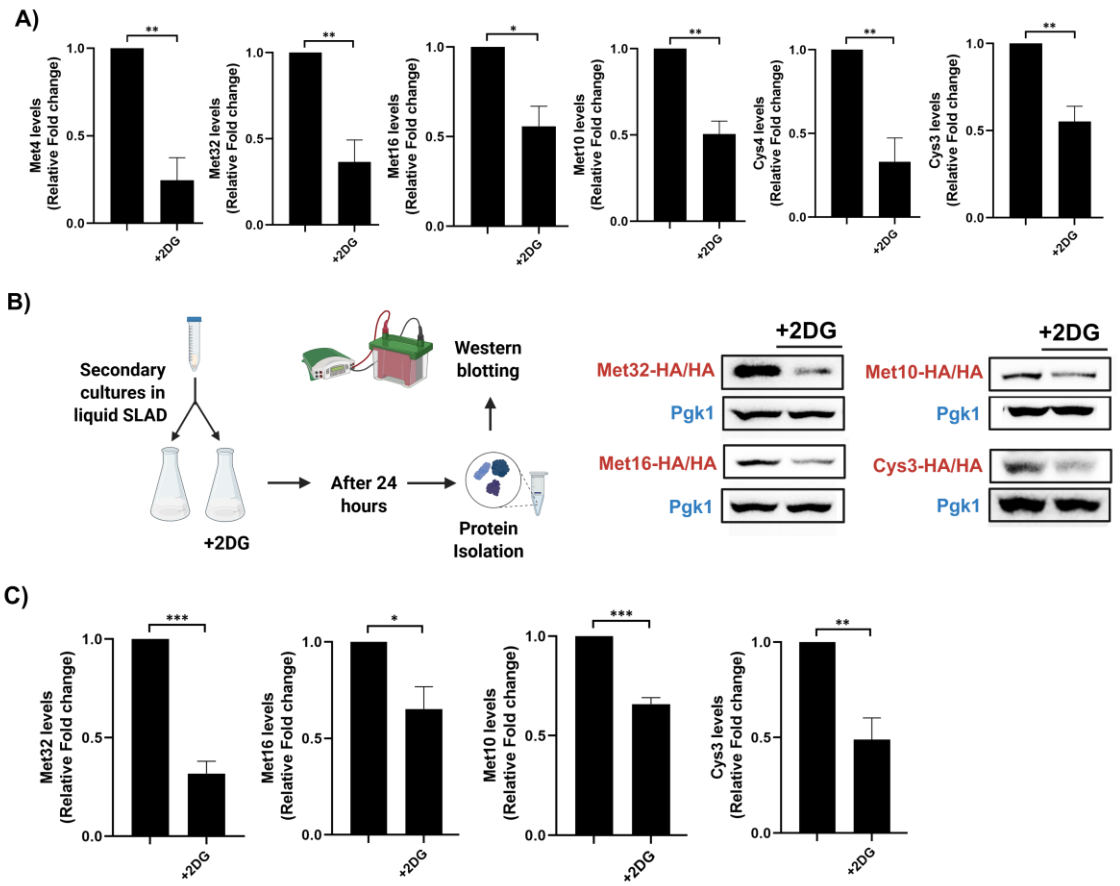

Figure Supplement 3. Expression of Proteins Involved in the *de novo* Biosynthesis of Sulfur-containing Amino Acids in Response to Glycolysis Perturbation.

(A) Epitope-tagged strains of various proteins involved in the *de novo* biosynthesis of sulfur-containing amino acids including Met4, Met32, Met16, Met10, Cys4 and Cys3 were spotted on SLAD in the presence and absence of sub-inhibitory concentration of 2DG following which, cells from colonies were isolated at day 5 and levels of these proteins were assessed using Western blotting. Raw images of Western blots were analysed using ImageJ to normalize targeted protein expression with the expression of housekeeping protein- β-actin, in order to generate densitometric graphs. Statistical analysis was done using unpaired t-test, **(P<0.01) and *(P<0.05). Error bars represent SEM. **(B)** Epitope-tagged strains of various proteins involved in the *de novo* biosynthesis of sulfur-containing amino acids including Met32, Met16, Met10 and Cys3 were grown in liquid SLAD and then treated with sub-inhibitory concentration of 2DG for 24 hours after which protein expression was checked using Western blotting (n=3). Pgk1 was used as loading control. **(C)** Raw images of Western blots were analysed using ImageJ to normalize targeted protein expression with the expression of housekeeping protein- Pgk1, in order to generate densitometric graphs. Statistical analysis was done using unpaired t-test, ***(P<0.001), **(P<0.01) and *(P<0.05). Error bars represent SEM.

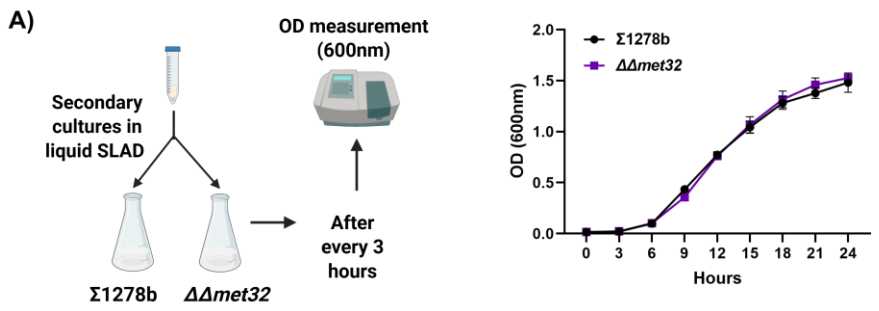

Figure Supplement 4. Monitoring of Overall Growth Rate of *ΔΔmet32* Strain.

(A) Growth curve analysis was performed to monitor overall growth of wild-type and *ΔΔmet32* knockout strain on SLAD. Overnight grown cultures of deletion strain (*ΔΔmet32*) along with wild-type strain (Σ1278b) were diluted to OD_{600}=0.01 in fresh SLAD and allowed to grow at 30 °C for 24 hours. OD_{600} was recorded at 3-h intervals.

Figure Supplement 5. Confirmation of *pfk1* Deletion in *C. albicans*.

(A) Confirmation of *ΔΔpfk1* strain using whole genome sequencing. IGV software (version 2.16.2) was used for data visualisation. Red box represents gene locus of *pfk1* in wild-type (SC5314) and *ΔΔpfk1* strains.

2006 **Supplemental Table 1. Yeast Strains Used in this Study**

2007

Strain	Genotype
***S. cerevisiae* Σ1278b**	
Wild-type	*MATa/α*
SV18	*Δadh1::G418/Δadh1::HygB MATa/α*
SV21	*Δpfk1::HygB/Δpfk1::G418 MATa/α*
SV270	*Δmet32::NAT/Δmet32::G418 MATa/α*
SV320	*MET32-HA::G418/MET32-HA::NAT MATa/α*
SV394	*CYS3-HA::NAT/CYS3-HA::G418 MATa/α*
SV395	*CYS4-HA::NAT/CYS4-HA::G418 MATa/α*
SV402	*MET10-HA::NAT/MET10-HA::G418 MATa/α*
SV404	*MET16-HA::NAT/MET16-HA::G418 MATa/α*
SV451	*MET30-HA::NAT/MET30-HA::G418 MATa/α*
SV461	*MET4-HA::NAT/MET4-HA::G418 MATa/α*
SV463	*Δmet30::HygB/MET4-HA::NAT/MET4-HA::G418 MATa/α*
SV473	*MET16-HA::NAT/MET16-HA::G418/Δmet30::HygB MATa/α*
SV475	*MET32-HA::G418/MET32-HA::NAT/Δmet30::HygB MATa/α*
SV476	*CYS3-HA::NAT/CYS3-HA::G418/Δmet30::HygB MATa/α*
***S. cerevisiae* CEN.PK**	
Wild-type	*MATa/α*
SV109	*Δadh1::G418/Δadh1::NAT MATa/α*
SV117	*Δpfk1::NAT/Δpfk1::G418 MATa/α*
***C. albicans* SC5314**	
Wild-type	*MATa/α*
SV308	*Δpfk1::FRT/Δpfk1::SAT-FLP MATa/α*

2008

2009 **Supplemental Table 2. Oligonucleotides Used in this Study**

2010

Oligonucleotides	Sequence (5′ to 3′)
Primers for *S. cerevisiae* Gene Editing and Genotyping	
ADH1 KO F1	AGCTATACCAAGCATACAATCAACTATCTCATATACAATGCGGATCCCCGGGTTAATTAA
ADH1 R1	ATTTAATAATAAAAATCATAAATCATAAGAAATTCGCTTAGAATTCGAGCTCGTTTAAAC
ADH1 KO Chk	CGTTGTTGTCTCACCATATC
PFK1 KO F1	TTTTATATAAAAAATCTGAAACAAAATCATATCAAAGATGCGGATCCCCGGGTTAATTAA
PFK1 R1	CTCCTTTTGCTTAACTTAAACTTTTCATTGCAATCATTCAGAATTCGAGCTCGTTTAAAC
PFK1 KO Chk	AGGATGAGAAAGTGAAATCG
MET32 C tag F1	TCATCGTCAAGATAACAACCACAATGGTAGCAGTAATGGCCGGATCCCCGGGTTAATTAA
MET32 R1	ATTTTCTTATTTGAGAAGATACACGCTATTTACTCTTTCAGAATTCGAGCTCGTTTAAAC
MET32 C tag Chk	GATGGTTTTTCGTCCCTTAC

Cys3 C tag F1	TTTGGAAGACATCAAGCAAGCCTTGAAACAAGCCACCAACCGGATCCCCGGGTTAATTAA
Cys3 R1	AAAGGTCCGGTCGAAGGCAGAGACGTGGCACTGGCGATTAGAATTCGAGCTCGTTTAAAC
Cys3 C tag Chk	CAGAGGTTTGAAGACTTTGC
Met10 Ctag F1	AGAATTAAAGGAAGCATCAAGATACATTTTAGAAGTCTACCGGATCCCCGGGTTAATTAA
Met10 R1	ACTGCTTTTCCTCGAGGTCACCCAAATATACAACGAGATGCGGATCCCCGGGTTAATTAA
Met10 Ctag Chk	TGGTTTAGGTACTGGTTTGG
Met16 Ctag F1	TGAAGCCAGCCGATTCGCGCAATTTTTAAAGCAAGATGCCCGGATCCCCGGGTTAATTAA
Met16 R1	GTCACATACATATGGTTATATATCGTACTCTATCTATCTAGAATTCGAGCTCGTTTAAAC
Met16 Ctag Chk	AATACGGGGATTTCTTATGG
Met4 Ctag F1	AAGCTTAAAGAAGCAAATTTTTGAGAAGGTTCAGAAAGAACGGATCCCCGGGTTAATTAA
Met4 R1	TATATATATATATAATTAAACTGTATAGTCTGTTATTTTAGAATTCGAGCTCGTTTAAAC
Met4 Ctag Chk	GAGCCAACTTTAAATGCAAG
Cys4 Ctag F1	CCATATCGTTACTAAGATGGATTTACTGAGCTACTTAGCACGGATCCCCGGGTTAATTAA
Cys4 R1	TTCTATGTTTGCTTTTATTTGAAGCGTGGGTTCTTATTTAGAATTCGAGCTCGTTTAAAC
Cys4 Ctag Chk	TTAAGGAAACCGCTAAGGTC
Met30 KO F1	AGGGGTGTGTGTTTGGTGATTTATAAAGGAGAAGGGCATGCGGATCCCCGGGTTAATTAA
Met30 R1	CGGATGTTTTTGACCAAGAAAAGACCACACACAGGTCCTAGAATTCGAGCTCGTTTAAAC
Met30 KO Chk	AGAGATAACTGCAGGGTGTG
Met30 Ctag F1	ATTTGGGTGCGTAAAAATGTACAAATTCGATCTCAATGATCGGATCCCCGGGTTAATTAA
Met30 Ctag Chk	AGGATGACCCAACAATGAC
Primers for *C. albicans* Gene Editing and Genotyping	
Psfs2a PFK1 F1	ATTTGAATAGCTTTTTCTTATTATTGAATTCTTTAATTTATCGTTTATTGCAAACAATCAATTATTCCTTATTATTTTGGGCAGATAACGAATTAGAAATGAAGTTCCTATACTTTCTAG
Psfs2a PFK1 R1	CAACACATTGAATTACATATATGAGTATAAAAAATCAAACTATACTGGGGACTACAAATCTTACTATTTTACACAACTCCTTATCTTCTGTTCTTCATTTGAAGTTCCTATTCTCTAGAA
Psfs2a SAT-FLP F1	AACATTGGATGCTGAGAACC
Psfs2a SAT-FLP R1	GCACATAATGCTATTTTCTC
PFK1 ApaI UF1	GAGAGGGCCCGTGATGCCTAACTTCTTGGT
PFK1 SacII DR1	CTCTCCGCGGTAGGCTGAATTGCTCGTATG
Pfk1 KO R1 Chk	GTACCAATTGAAGTACCACC
FRT F1	CTTTCTAGAGAATAGGAACT

FRT R1	AGTTCCTATTCTCTAGAAAG
Primers for RT-qPCR	
Candida Act1 F1	TTGGATTCTGGTGATGGTGTTA
Candida Act1 R1	TCAAGTCTCTACCAGCCAAATC
Candida Met32 F1	CACCAACACAACACCATCAAC
Candida Met32 R1	TCCAATTCCACCACCAGTAATC
Candida Met3 F1	GTTCCAACAACAAACCCAACTC
Candida Met3 R1	TCACCATCAGCATTACCAGAAG
Candida Met14 F1	GTTGCTGAACAAAGAGATCCAAA
Candida Met14 R1	CCTGAATGGTTCTTAACGTGTATTT
Candida Met16 F1	GAGTTTCGGCTGTGCTAACT
Candida Met16 R1	TTCCACTTGTTTCCTCGTATTCT
Candida Met5 F1	TTTATGGTGCGTGTTCGTTTAC
Candida Met5 R1	TAGCCCTGGTGGTCAATTTC
Candida Met10 F1	GGGTTGATCCAAAGGGAAGAT
Candida Met10 R1	GACAATGGTGGCAACTTCATAAC
Candida Met17 F1	TCAAGGACATCACCAACACC
Candida Met17 R1	CTTAGAGTCACCCACATTAGCC
Candida Cys3 F1	TCGCCATACCTTTCCAATCC
Candida Cys3 R1	GGTTGCCAAGACTCCCATAA
Candida Als3 F1	GGTGGCACTGATTCGGTTAT
Candida Als3 R1	GCGGTAATGGTAGTGGTAGTTG
Candida Ece1 F1	TTGGCAACATTCCACAAGTAATC
Candida Ece1 R1	CAGCAATGATACCAGCAACAAC
Candida Hwp1 F1	CTCTACGACTGAAGGTGCTATTC
Candida Hwp1 R1	GTAGAAATAGGAGCGACACTTGA
Candida Hyr1 F1	CACATCAAGTCCTGGTCAATCTA
Candida Hyr1 R1	TGGAACAGTGGTGAAGATAGTG
Candida Ihd1 F1	GGCTCTCAAGGTCAATCTACAA
Candida Ihd1 R1	ACTAGCACCATCGTTACCATTAG
Candida Rbt1 F1	CCATCTGCTAACTCCTCATACAC
Candida Rbt1 R1	CAAGAATGCAGCAAGACCAATAA
Candida Sap6 F1	GAGTGTTCTTGCTTTCGCTTTAT
Candida Sap6 R1	CATCTGGATCAACAAGGGATCT

2011
2012 **Supplemental Table 3. List of Reagents and Tools Used in this Study**
2013

Reagents/ Resource	Reference or Source	Identifier or catalog Number
Recombinant DNA		
pFA6a-kanMX	Gift from Dr. Sunil Laxman	Not applicable
pFA6a-Hyg	Gift from Dr. Sunil Laxman	Not applicable
pFA6a-Nat	Gift from Dr. Sunil Laxman	Not applicable

pFA6a-Ctag-HA-G418	Gift from Dr. Sunil Laxman	Not applicable
pFA6a-Ctag-HA-NAT	Gift from Dr. Sunil Laxman	Not applicable
pSFS2a-NAT	Gift from Dr. Kaustuv Sanyal	Not applicable
Antibodies		
Rabbit anti-HA	Cell Signaling Technology	3724S
Mouse anti-β-actin	Cell Signaling Technology	3700
Mouse anti-PGK1	Santa Cruz Biotechnology	sc-130335
Goat anti-Rabbit IgG-HRP conjugate	Cell Signaling Technology	7074S
Horse anti-Mouse IgG-HRP conjugate	Cell Signaling Technology	7076S
Chemicals, enzymes and other reagents		
BD Bacto agar	Becton Dickinson	214010
Agarose	MP Biomedicals	100267
Ammonium sulfate	Sisco Research Laboratories	0149175
Blotto, non-fat dry milk	Santa Cruz Biotechnology	sc-2324
B-mercaptoethanol	Sigma-Aldrich	444203
Diluent	HiMedia	MB228
D-(+)-Glucose anhydrous	HiMedia	GRM016
Lithium acetate	Sigma-Aldrich	517992
Peptone	Thermo Fisher Scientific	211677
RNaseZAP	Sigma-Aldrich	R2020
SDS	G Biosciences	RC1184
Trichloro acetic acid	Sigma-Aldrich	100807
Tris, free base	HiMedia	MB029
Tween 20	Sigma-Aldrich	P7949
Yeast extract	Thermo Fisher Scientific	212750
Yeast nitrogen base w/o amino acids and ammonium sulfate	Becton Dickinson	233520
D-Sucrose	HiMedia	GRM3063
D-Fructose	Sigma-Aldrich	F3510
D-Maltose	Sigma-Aldrich	M5895
D-Mannose	Sigma-Aldrich	63580
D-Trehalose	Sigma-Aldrich	T0167
D-Galactose	Sigma-Aldrich	48260
L-Cysteine	Sigma-Aldrich	30089
L-Methionine	Sigma-Aldrich	64319
DL-Glyceraldehyde	Sigma-Aldrich	G5001
Sodium citrate	Sigma-Aldrich	C8532
Glycerol	HiMedia	MB060
Potassium acetate	MP Biomedicals	191425
2-Deoxy-D-Glucose	Sigma-Aldrich	D8375
NAT	Jena Bioscience	AB-102XL
G418	MP Biomedicals	158782
Ethidium bromide	HiMedia	MB074
Pico-ECL substrate	Thermo Fisher Scientific	34579
Femto-ECL substrate	Thermo Fisher Scientific	34094

TEMED	Sisco Research Laboratories	52145
Hygromycin	Sigma-Aldrich	H0654
Ribopure RNA purification kit-Yeast	Thermo Fisher Scientific	AM1926
BCA Protein Assay kit	Thermo Fisher Scientific	23227
GMS Staining kit	ABcam	AB287884
Softwares		
RStudio v4.3.2	Posit	Not applicable
GraphPad Prism v9	GraphPad software	Not applicable
ImageJ		Not applicable
IGV v2.16.2		Not applicable
Other		
Glass beads	HiMedia	GRM2228
MATRIX thermoshaker	IKA	Not applicable
Spectrophotometer	Thermo Fisher Scientific	Not applicable
Proflex PCR systems	Thermo Fisher Scientific	Not applicable
MVX10 Stereo Microscope	OLYMPUS Scientific	Not applicable
Biosafety Cabinet	IGene Labserve	Not applicable
PVDF membrane	Milipore	IPVH00010
Mini Trans-Blot Cell Module	Bio-Rad	Not applicable
ChemiDoc™ MP analyzer	Bio-Rad	Not applicable
QuantStudio Real-Time PCR System	Thermo Fisher Scientific	Not applicable
Apotome widefield fluorescence microscope	Zeiss	Not applicable
Centrifuge 5425R	Eppendorf	Not applicable

2014